BIOGAS REFORMATION OVER Pr-PROMOTED Ni/MgO

SHAIK ISMAIL BIN MOHAMED ALI

BACHELOR OF CHEMICAL ENGINEERING
UNIVERSITI MALAYSIA PAHANG

Thesis Access Form

No_____Location_____

Author: ……

Title: ……

Status of access OPEN / RESTRICTED / CONFIDENTIAL

Moratorium period:_____ years, ending_____/_____200____

Conditions of access proved by (CAPITALS): DR CHENG CHIN KUI

Supervisor (Signature)……

Faculty: ……

Author's Declaration: *I agree the following conditions:*

OPEN access work shall be made available (in the University and externally) and reproduced as necessary at the discretion of the University Librarian or Head of Department. It may also be copied by the British Library in microfilm or other form for supply to requesting libraries or individuals, subject to an indication of intended use for non-publishing purposes in the following form, placed on the copy and on any covering document or label.

*The statement itself shall apply to **ALL** copies:*

This copy has been supplied on the understanding that it is copyright material and that no quotation from the thesis may be published without proper acknowledgement.

Restricted/confidential work: All access and any photocopying shall be strictly subject to written permission from the University Head of Department and any external sponsor, if any.

Author's signature……Date: ……

users declaration: for signature during any Moratorium period (Not Open work): ***I undertake to uphold the above conditions:***			
Date	Name (CAPITALS)	Signature	Address

BIOGAS REFORMATION OVER Pr-PROMOTED Ni/MgO

Shaik Ismail Bin Mohamed Ali

Thesis submitted in partial fulfilment of the requirements
for the award of the degree of
Bachelor of Chemical Engineering

Faculty of Chemical & Natural Resources Engineering

UNIVERSITI MALAYSIA PAHANG

JUNE 2014

SUPERVISOR'S DECLARATION

I hereby declare that I have checked this thesis and in my opinion, this thesis is adequate in terms of scope and quality for the award of the degree of Bachelor of Chemical Engineering.

Signature :
Name of main supervisor : DR. CHENG CHIN KUI
Position : SENIOR LECTURER
Date : 2nd JULY 2014

STUDENT'S DECLARATION

I hereby declare that the work in this thesis is my own except for quotations and summaries which have been duly acknowledged. The thesis has not been accepted for any degree and is not concurrently submitted for award of other degree.

Signature :
Name : SHAIK ISMAIL BIN MOHAMED ALI
ID Number : KA10083
Date : 2nd JULY 2014

Dedication

To my parents for their support, love, dream and sacrifice throughout my life.

ACKNOWLEDGEMENT

First and foremost, I would like to thank God for His blessings for giving me patience and good health throughout the duration of this thesis. I am very honoured and grateful to Dr Cheng Chin Kui for being my supervisor. His advises and comments have been a great contribution for the achievement of my research. I would like to extend my gratitude to my course mates who have been kind in sharing knowledge and time to help me with my report. I really appreciate it. My sincere thanks go to all my lab mates and members of the staff of the Chemical Engineering and Natural Resources Faculty, UMP, who helped me in many ways and made my stay at UMP pleasant and unforgettable.

ABSTRACT

Promoting rare earth element into commercial catalyst has become interesting research in designing the best catalyst for methane dry reforming. 1wt%, 3wt% and 5wt% Pr loadings into Ni/MgO were prepared by wet-impregnation method and calcined at 973 K. The prepared catalyst was characterized using N_2physisorption, field emission scanning electron microscopy (FESEM), X-ray diffraction spectroscopy (XRD) andenergy dispersive X-ray spectroscopy (EDX). The BET surface area increasedwhen the Pr loading percentage was increased. The surface area for 1wt% Pr loading of Pr-Ni/MgO was 14.3 m^2/g and 28.11 m^2/g for 5wt% Pr loading. The structure of the 5wt% Pr promoted Pr-Ni/MgO was much closely packed compared to the non-promoted Ni/MgO that captured by FESEM. Furthermore, XRD peak shows no peak of PrO for 5% Pr-Ni/MgO as the interaction was strong and well dispersed that didn't allow the XRD to detect. This statement was further supported by EDX result that showed the Pr was well dispersed on the catalyst. The MgO peak was found at 28.34^o, 37.02^o, 42.99^o, 62.99^o, 62.40^o, 74.85^o and 78.83^o. Reaction studies over the Pr-Ni/MgO showed that the 5wt% promoted consistently yielded the best reaction at 1073, 1123 and 1173 K respectively. The conversion can reach ca. 61.44 % at 1173K when reactant volumetric flow ratio, CO_2/CH_4 was fixed at unity. In addition, the product H_2/CO ratioswere found to be less than 3.0 which were similar to the values reported in most of the other studies. The reaction power order for the CH_4 and CO_2 was 0.6111 and 0.4274 respectively whilstthe activation energy and activity for the reaction over 5wt% Pr-Ni/MgO catalyst was 66.10kJ/mol and 0.372.

Keywords: Catalyst, syngas, methane dry reforming, activation energy, activity

ABSTRAK

Penggalakkan unsur Nadir bumi ke dalam pemangkin komersial telah menjadi penyelidikan yang menarik dalam mereka bentuk pemangkin terbaik untuk reformasi kering metana. Promosi berat 1%, 3% dan 5% Pr ke dalam Ni/MgO telah disediakan mengunakan kaedah basah-impregnasi dan dikalsinasikan pada 973 K. Pemangkin yang disediakan, disifatkan menggunakan physisorpsi N_2, pelepasan bidang mengimbas microscopy elektron (FESEM), Spektroskopi belauan sinar-x (XRD) dan tenaga dispersive X-ray spektroskopi (EDX).). Luas permukaan BET meningkat apabila peratusan berat Pr yang dimuatkan meningkat. Luas permukaan untuk pemangkin yang dipromotkan 1% Pr-Ni/MgO ialah 14.3 m^2/g dan 28.11 m^2/g bagi 5% Pr-Ni/MgO. Struktur pemangkin 5% Pr dalam Pr-Ni/MgO dibandingkan dengan Ni/MgO yang tidak dipromotkan Pr adalah lebih rapat didapati dari FESEM. Selain itu, kemuncak XRD menunjukkan tiada puncak bagi PrO dalam 5% Pr-Ni/MgO kerana interaksi kuat terhadap pemangkin yang tidak membenarkan XRD untuk mengesan. Kenyataan ini seterusnya disokong oleh EDX yang menunjukkan Pr yang tersebar baik pada pemangkin. Puncak MgO didapati pada 28.34º, 37.02º, 42.99º, 62.99º, 62.40º, 74.85º dan 78.83º. Kajian tindak balas ke atas semua pemangkin Pr-Ni/MgO menunjukkan bahawa 5 % Pr yang dipromotkan kepada Pr-Ni/MgO memberi hasil tindak balas terbaik pada suhu 1073 K, 1123K dan 1173K. Penukaran methana mencapai 61.44% pada suhu 1173 K apabila nisbah aliran isipadu CO_2/CH_4 ditetapkan pada satu. Di samping itu, nisbah produk H_2/CO didapati kurang dari 3.0 yang mirip kepada nilai yang dilaporkan dalam kebanyakan kajian lain. Perintah kuasa reaksi untuk CH_4 dan CO_2 didapati 0.6111 dan 0.4274. Manakala tenaga pengaktifan dan aktiviti bagi tindak balas ke oleh pemangkin yang dipromotkan 5% Pr-Ni/MgO adalah 66.10 kJ/mol dan 0.372.

TABLE OF CONTENTS

LIST OF FIGURES

LIST OF TABLE

LIST OF ABBREVIATIONS

Pr	: Praseodymium
C	: characteristic constant of the adsorbate
D	: inter plane distance of crystal
$d_{spacings}$	: interplanar distance
D	: crystalline size
Ea	: activation energy
k_{Sch}	: Scherrer constant
n	: order of reflection (integer)
P	: gas pressure
Ps	: saturation pressure of the adsorbate gas
P/Po	: relative pressure
r_k	: pore radius
R	: gas constant
T	: temperature
V	: volume of gas adsorbed
V_m	: volume of gas adsorbed corresponding to monolayer coverage
vm	: liquid molar volume
DRM	: Dry reforming of methane
POM	: Partial Oxidation of Methane
ppm	: Part per million

CHAPTER 1

INTRODUCTION

1.1 Introduction

Crude palm oil demand is growing tremendously in Malaysia and accounted as among the world largest palm oil producer. It is a well-known fact that palm oil has higher yield of production per hectare than the other oil seed crops including soybeans (Chin et al., 2013), hence its relatively lower price compared to the other oil and burgeoning demand. Although crude palm oil industry is expanding tremendously, it produces significant amount of palm oil mill effluent (POME) from crude palm oil mills. POME is acidic typified by its pH of 4 to 5 (Rupani et al., 2010). Significantly, POME degradation contributes to greenhouse gases such as CO_2, CH_4, NO_X, HFC, per-fluorocarbon and SF_6 which are detrimental to weather pattern (Kaewmai et al., 2012). Further studies also found that H_2S amount was very low (< 2000 ppm) while CH_4 (65%) and CO_2 (35%) constitute the highest proportion (Yacob et al., 2005). Therefore, POME treatment could be considered to become part of greenhouse effect contributor.

In the current practice, biogas is used as feed for electricity generation. However, the substantial amount of CO_2, which is a natural fire-repellent, decreases the efficiency of combustion (Yacob et al., 2005). Alternatively, biogas reformation reaction is proposed in the current work, which involves the reaction of CO_2 with CH_4 over specific catalysts. Significantly, there are three methods of reaction found in literature viz. steam reforming of methane (SRM), dry reforming of methane (DRM) and partial oxidation of methane (POM) (Meshkani et al., 2013). Biogas reformation is the reaction between CO_2 and CH_4 to produce synthesis gas (syngas), a mixture of CO and H_2 vital as an intermediate reactant for Fisher-Tropsch synthesis to produce liquid hydrocarbon. In order to fully utilize the biogas from POME, dry reforming of CH_4 (DRM) is a wise pathway as these two reactants are readily available as main components of biogas. Furthermore, Fisher-Tropsch synthesis requires H_2:CO composition of less than 3.0

(Meshkani et al., 2013). In some literatures, it were claimed that dry reforming of methane produced syngas with H_2:CO composition ratio that met the requirement (Meshkani et al., 2013). Basically, Ni, Pt, Rh and Ru exhibit good activity in dry reforming of methane (DRM) (Meshkani et al., 2013). However, those metal are expensive and rarely available. It is found that, ruthenium catalyst shows the best activity among other transition catalyst (Zhang et al., 2013). Although Ru is very good catalyst for reformation of CH_4, the price is not suitable for the industrial application. Thus, the researchers choose the cheapest metal and test them accordingly to obtain the best catalyst for the highest conversion of the biogas. Co, Ni and Fe were in the list of more economical catalysts. From literature, Ni found to give the highest conversion among three of the catalyst (Meshkani & Rezaei, 2011).

Therefore, Ni is selected as the suitable catalyst for biogas reformation. Dry reforming of methane is an endothermic reaction conducted with Ni catalyst to give high conversion of methane. However, the major drawback of this reaction is catalyst deactivation. Catalyst deactivations refer to the loss of catalytic activity or selectivity toward time. There are two major factors contribute to catalyst deactivation in this reaction which is by carbon deposition and/or sintering. Carbon deposition means, the carbon deposited onto the actives site of Ni and reduces the site for reaction on the catalyst. Sintering is the process of Ni growth in size that reduces the specific surface area of catalyst. Sintering mostly affected by the temperature of the reaction. Carbon deposition can occur either by methane cracking or carbon monoxide decomposition. These reactions produce solid carbon and deposited onto the actives site of the Ni catalyst. Since it is harder to control the reaction of carbon formation, catalyst support was introduced. Carbon deposition mostly favours acidic surface to accept electron and deposit onto the catalyst surface. Therefore, alkaline earth metal oxides were introduced to reduce the surface acidity of the catalyst and furthermore promoting electron species also included to retard the carbon formation. This study is about preparing Ni supported on magnesium oxide promoted by praseodymium oxide in dry reformation of biogas reaction.

1.2. Motivation

Since the crude palm oil (CPM) production increases every year, the more palm oil mill effluent (POME) being produced. Thus, it's indirectly increases the amount of biogas release to atmosphere while POME being treated. So, it is necessary to convert this gas into synthesis gas as way to curb excessive emission of greenhouse gases. As aforementioned, biogas reforming remains the only reaction that utilizes the entire biogas without a need to purify the biogas. Previously, many catalyst studies have been carried out to obtain the best reforming catalyst and mostly showed Ni as the best candidate although it was also found that it was prone to deactivation. Therefore, to mitigate this issue, alkaline earth metal oxide as support was employed. In some studies, Ni support limited to aluminium based. Therefore, to increase the basicity of the catalyst surface alkaline earth metal oxide like magnesium oxide with Praseodymium oxide promoter could be best choices in this study.

1.3. Objectives

This research is to prepare the Pr-Ni/MgO catalyst with different amount of praseodymium oxide and to study the biogas reforming performance.

1.4. Scope of study

To achieve the objectives, several tasks were carefully implemented:

I. Catalyst preparation and characterization

Catalyst preparation was a vital part of the research. Ni/MgO catalyst promoted with different amounts of Praseodymium oxide were prepared by impregnation method. Then, the catalyst were characterized using some equipment such as:

1. Brunauer – Emmett –Teller (BET)
2. X-ray Diffraction (XRD)
3. Field Emission Scanning Electron Microscopy (SEM)
4. Energy Dispersive X-ray (EDX)

II. Reaction

DRM was conducted in packed bed reactor at atmospheric pressure with different temperature and reactant flow ratio. Screening conducted at CO_2/CH_4 volumetric ratio of 1:1 at 1073K, 1123K, and 1173K. The reaction temperature selection for the best performed catalyst was chosen within the screening process.

Summary

Dry reforming methane is very essential to reduce the greenhouse effect that contributed by palm oil mill effluent decomposition. This reaction is the only reaction utilized the major product component from the POME decomposition. Choosing the best catalyst for this particular reaction must be precisely investigated with previous study. Ni metal is the best choice of active sites for industrial application purpose. Since introducing alkaline support could benefit the reaction stability. MgO chosen as the best choice of carrier for this particular catalyst. In order to increase further the reaction conversion of methane and the stability of the catalyst, Pr is promoted into the catalyst to study the activity of the catalyst.

CHAPTER 2

LITERATURE REVIEW

2.1 Introduction

Synthesis gas is a very crucial raw material for many downstream chemicals such as ammonia, methanol, dimethyl ether and most importantly the increasingly-demanded synthetic fuel by Fisher-Tropsch reaction plant (Aasberg-Petersen et al., 2011). POME upon decomposition would release abundant quantity of CH_4 and CO_2 with traces amount of H_2S (Yacob et al., 2005). Significantly, there are three routes of reaction to produce synthesis gas, viz. methane steam reforming, methane dry reforming and partial oxidation of methane (Meshkani et al., 2013). Methane steam reforming is the most commonly found reaction in many industries with the reaction as given by:

$$CH_4 + H_2O \leftrightarrow CO + 3H_2 \qquad \Delta H^0_{298} = 205.8 kJ mol^{-1} \tag{2.1}$$

As for more general hydrocarbon,

$$C_nH_m + nH_2O \leftrightarrow nCO + (n + \frac{1}{2}m)H_2 \quad \Delta H^0_{298} = 498.6\, kJ\, mol^{-1} (for\ C_3H_8) \tag{2.2}$$

Practically, methane steam reformation uses steam and methane as reactant to produce synthesis gas. This reaction is an endothermic reaction that requires external energy supply to conduct that particular reaction.

The second route of reaction is known as carbon dioxide reforming or methane dry reforming. This reaction uses CO_2 instead of steam to produce syngas. The reaction is given by

$$CH_4 + CO_2 \leftrightarrow 2CO + 2H_2 \qquad \Delta H^0_{298} = 247.0\, kJ\, mol^{-1} \tag{2.3}$$

Methane dry reformation is an endothermic reaction that uses CH_4 and CO_2 as the reaction feed. Unlike the two previous routes, partial oxidation is mildly exothermic reaction, which releases heat for each converted methane. The reaction equation given by,

$$CH_4 + \frac{1}{2}O_2 \leftrightarrow CO + 2H_2 \qquad \Delta H_{298}^0 = -36.0\, kJ\, mol^{-1} \tag{2.4}$$

There are some studies that conduct combination of dry reforming of methane and partial oxidation (Meshkani et al., 2013). This would be very useful as the heat released from the partial oxidation can be utilized for the dry reforming of methane as it requires energy (Meshkani et al., 2013). Furthermore, this reaction can tune product gas flow rate ratio for H_2:CO to desirable ratio (Meshkani et al., 2013). However, to fully utilize the biogas, methane dry reforming could be the best choice as envisioned by the current study. In some literature also had stated that, the product gas flow rate ratio H_2: CO from dry reforming of methane is less than 3, which is suitable for Fisher-Tropsch synthesis.

2.2 Catalytic dry reforming of hydrocarbon

Dry reforming of methane is very appealing reaction that desires the industry to produce synthesis gas. It combines CH_4, which is the principal component of energy source, and CO_2 the greenhouse gas (Deutschmann, 2011). This reaction also very interesting as it uses methane and carbon dioxide, which is cheap feedstock that available abundantly from POME. Therefore, this is good alternative for steam reforming, which is used to produce synthesis gas. Furthermore, dry reforming of methane produces suitable product ratio of $H_2 : CO$ which is less than 3. This kind of product ratio is very suitable for Fischer-Tropsch synthesis of liquid hydrocarbon (Meshkani & Rezaei, 2011). In addition, the couple of dry reforming of methane and Fischer-Tropsch synthesis could be very useful as the heat from the Fischer-Tropsch reaction can drive the dry reformation of methane reaction to minimize the energy cost (Ni et al., 2013). Currently, many studies being conducted to improve this reaction by using catalyst. However, the major problem on the catalyst studies of this reaction is coking and sintering. One of the most recent studies is to avoid the coking by exploring the alkaline

earth metal oxide as the catalyst support for that particular reaction. In order to practically apply this reaction in industry, Ni catalyst was chosen as the catalyst. Ni catalyst is the best and cheap catalyst that is being used in recent industry to conduct dry reforming of methane.

The dry reforming of methane is given by,

$$CH_4 + CO_2 \leftrightarrow 2CO + 2H_2 \qquad \Delta H_{298}^0 = 247.0\,kJ\,mol^{-1} \tag{2.5}$$

While carbon deposition may occur via, methane decomposition

$$CH_4 \rightarrow C(s) + 2H_2 \tag{2.6}$$

Or CO disproportionation (Boudouard) reaction,

$$2CO \leftrightarrow C + CO_2 \tag{2.7}$$

2.2.1 Kinetics

Kinetics study is very important to explain the nature of the reaction. Kinetics study is mainly function of support type, hydrocarbon nature and reaction condition (temperature and pressure) (Al-Ubaid, 1986). It is very expected that, methane dry reforming kinetics study being conducted extensively as it is cheap and abundantly available fuel gas from POME. A kinetic study on dry reforming of methane conducted by using $LaSrNiO_4$ (Pichas et al., 2010). In their study, the reaction temperature was conducted in range of 633K-713K at atmospheric pressure. Surface reaction between adsorbed methane and adsorbed carbon dioxide is considered as the rate determining steps. It was found that, the reaction order with respect to CH_4 be in range of 0.41– 0.89 and the reaction order respect to CO_2 found was approximately zero order. CH_4 conversion in this study found to be lower than carbon dioxide due to the water-gas shift reaction which given by,

$$CO_2 + H_2 \leftrightarrow CO + H_2O \qquad \Delta H_{298} = 46.1 kJ/mol \tag{2.8}$$

There is another study on the kinetics using molybdenum carbide as alternatives catalyst for dry reforming of methane. (LaMont and Thomson, 2004) reported that was

successfully study the kinetics of molybdenum carbide in dry reforming of methane by stabilizing the Mo_2C catalyst by co-feeding CO with the reactant gases. They obtain the activation energy of 42.1 kcal/mol with reaction order of 1 respect to methane and 0.7 respect to carbon dioxide. (Darujati & Thomson, 2006) also further investigate the effect of promoting ceria on the aluminium oxide supported molybdenum carbide catalyst, . They found that, the reaction order of dry methane reforming is 0.95 ± 0.04 for methane and -0.18 ± 0.03 for carbon dioxide. This study conducted with partial pressure range of 0.02 to 0.24 bar for methane and 0.02-0.31 bar for carbon dioxide and the rest is supply by argon to maintain at atmospheric pressure. The activation energy obtained from this result was 45.5 ±0.99 kcal/mol. There are another studies were conducted on the bimetallic catalyst. (Özkara-Aydınoğlu & Erhan Aksoylu, 2013)Studied the kinetics of 0.2 wt.%Pt-15wt.%Ni/∂-Al_2O_3 and 0.3wt. %Pt-10wt% Ni/∂-Al_2O_3 .They found that the activation energy of 0.3% Pt promoted catalyst is 26.9 kcal/mol and 26.6 kcal/mol for 0.2 % Pt promoted catalyst. The reaction for 0.3 % platinum promoted Ni catalyst is 1 respect to methane and 0.87 for carbon dioxide. For the 0.2 % promoted platinum is 1.09 respect to methane and 1.40 for carbon dioxide. (Özkara-Aydınoğlu & Erhan Aksoylu, 2013) Mentioned that the reaction order for lower platinum content catalyst increases the carbon dioxide reaction order. This is because the oxygen in the carbon dioxide is utilized to clean the carbon deposit. Even there are many kinetic studies conducted over nickel based catalyst, there were some argument regarding the mechanism of the dry reforming reaction. The rate limiting step for dry reforming of methane is CH_xO decomposition. This rate determining step was concluded by (Leo et al., 2000) and (Osaki & Mori., 2001). There are other mechanism also proposed by (Bradford & Albert, 1996) and (Nandini et al., 2006) whereby involves dissociative CH_4 adsorption and CH_xO decomposition. Another study by (Aparicio, 1997) also reported that further dissociation of CH_4 and CO desorption as rate determination steps. From all this proposed rate determination steps, (Cui et al., 2007) concluded that the rate determining steps depend on their particular reaction temperature. Therefore, they study on typical $Ni/\alpha - Al_2O_3$ catalyst at temperature range of 823 to 1023 K to study the effect of temperature on the reforming reaction mechanism. They found that, CH_4 dissociation was the rate determining step and CO

desorption also was found to be limiting reaction in temperature range of 823-848 K. Table 2.0 show the literature studies on methane dry reforming with Ni catalyst.

Table 2.1: Kinetics from some previous study

Authors	Catalyst	Hydrocarbon	Kinetics order		Activation Energy	
			CH_4	CO_2		
(Pichas et al., 2010)	$LaSrNiO_4$	CH_4	0.41-0.89	~0	41.8	kJ/mol
(Darujati & Thomson, 2006)	30% Mo_2C/Al_2O_3(3 wt% Ce)	CH_4	0.95 ±0.04	0.18 ±0.03	45.5 ± 0.99	kcal/mol
(Özkara-Aydınoğlu & Erhan Aksoylu, 2013)	0.2%.Pt-15%Ni/Al_2O_3	CH_4	1.09	1.4	26.9	kcal/mol
(Özkara-Aydınoğlu & Erhan Aksoylu, 2013)	0.3%.Pt-10%Ni/Al_2O_3	CH_4	1	0.87	26.6	kcal/mol

2.2.2 Reaction Associated with Dry Reforming of Methane

It is very rare that any organic compound does not undergo any further side reaction. There are some reaction occur while the dry reforming reaction is conducted. The reaction could be in series reaction or parallel reaction. Dry reforming associated reaction is water gas shift reaction, Boudouard reaction and methane decomposition.

2.2.2.1 Boudouard Reaction

One of the side reactions is the Boudouard reaction which also known as CO disproportionation, where CO may dissociate to produce CO_2 and surface carbon as:

$$2CO \leftrightarrow C + CO_2 \qquad \Delta H_{298}^{0} = -172.5 kJ/mol \tag{2.9}$$

Thermodynamically, this reaction is likely to occur at a reaction temperature lower than 972 K. However, the presence of high concentrations of CO_2 in the system may facilitate keeping the influence of this reaction to a minimum. Also, quicker removal for CO from the system should assist in reducing the effect of this side reaction. Boudouard reaction mechanisms had been extensively studied by (Tottrup, 1976) And they found the reaction mechanism as follow:

$$CO + * \leftrightarrow CO* \tag{2.10}$$

$$CO* + * \rightarrow C* + O* \tag{2.11}$$

$$CO* + O* \leftrightarrow CO_2* \tag{2.12}$$

$$CO_2* \leftrightarrow CO_2 + * \tag{2.13}$$

Where, * symbolized as the actives sites of the catalyst, CO*, C*, O*and CO_2* is the chemisorb species on the catalyst. Carbon monoxide produced from the dry reforming reaction adsorbed onto the catalyst actives sites by single site adsorption. Then, the adsorbed carbon dioxide dissociates onto another sites of the catalyst form two site with carbon and oxygen. The chemisorbed oxygen will react with another carbon monoxide to become carbon dioxide while the carbon atom become deposited onto the catalyst surface and reduces the number of actives sites. This causes the catalyst activity reduces over time. (Tottrup, 1976) mention in his study that the carbon dioxide have influence

on the methane decomposition at temperature above 300 ^{o}C. However, methane dry reforming is endothermic reaction, which favor high reaction temperature. Thus, increasing the carbon dioxide amount in the feed could be very useful to reduce this reaction to occur. The rate of carbon monoxide decomposition (Boudouard reaction) is given by,

$$r = k\frac{p_{co}}{\left(1+K_A p_{co}+K_B\left(p_{co_2}/p_{co}\right)\right)^2} \tag{2.14}$$

Based on the rate law also can be concluded that, the rate of Boudouard reaction is directly proportional to the partial pressure of carbon monoxide. Therefore, removing the correct amount of carbon monoxide could benefit the catalyst stability. However, the CO removal amount should not affect the methane reforming reaction to shift to reactant as it reversible reaction.

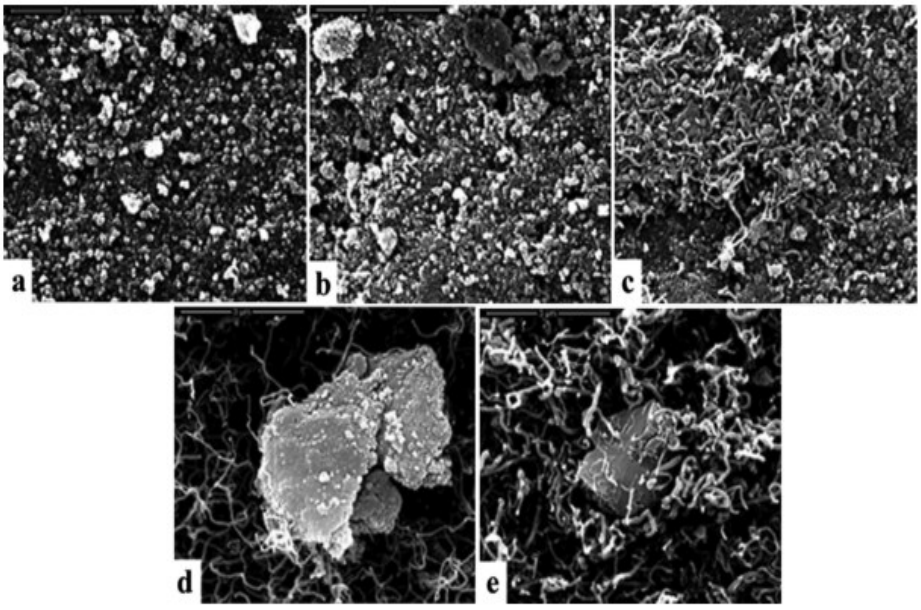

Figure 2.1: SEM images of Ni-Zr/SiO_2 catalysts after 10 h reaction at different temperature (a): 800 ^{o}C; (b): 750 ^{o}C; (c): 700 ^{o}C; (d): 650 ^{o}C; (e): 600 ^{o}C.

Figure 2.1 show an example of carbon deposition images of Ni-Zr/SiO_2 at different temperature. According to (Yao et al., 2013), at low temperature vermicular type carbon was observed and at high temperature, the vermicular carbon deposition was not found. This suggest that, the vermicular type carbon formation over this Ni-Zr/SiO_2 catalyst could be avoided if the reaction temperature is over 750 ^{o}C. This is one of the type of

carbon formation on Zr promoted catalyst. Each type of catalyst could give different structure of carbon deposition.

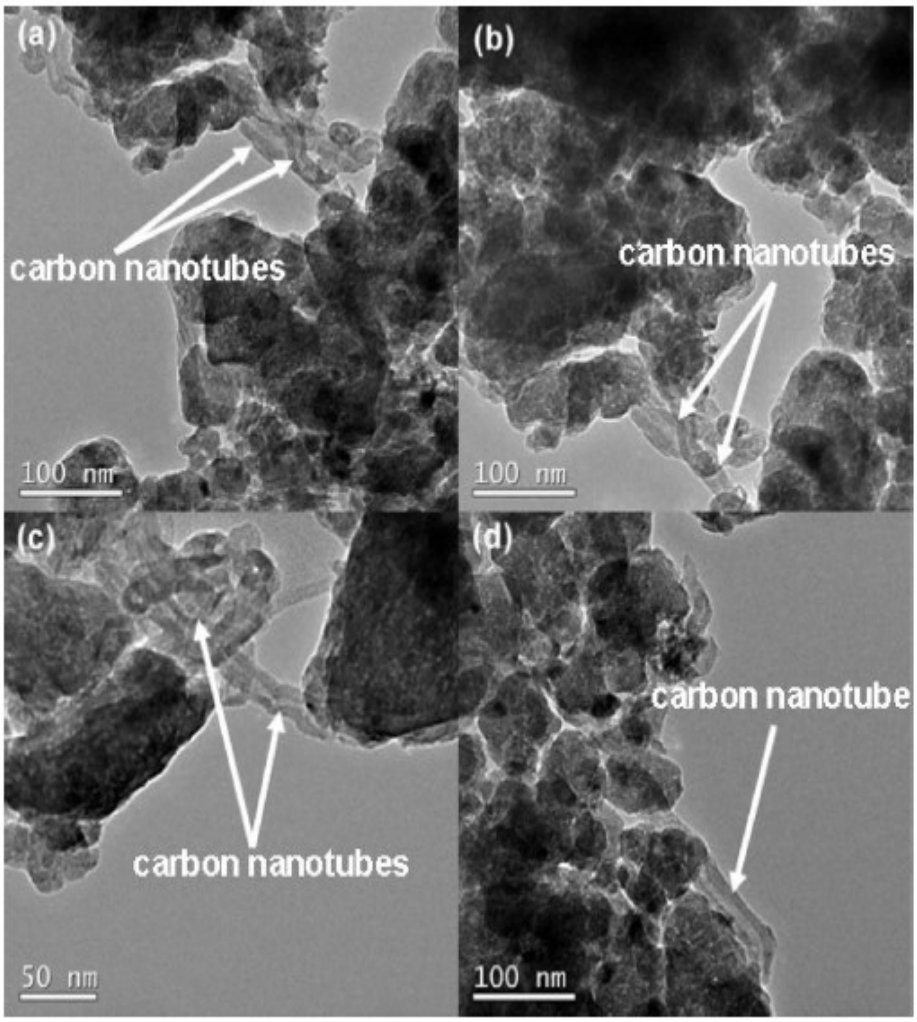

Figure 2.2: TEM images of the 50 h endurance-tested M-5Ni3Ce92Al catalyst

Figure 2.2 showing the TEM images on the carbon deposition mesoporous 3%Ce-5%Ni/92%Al studied by (Xu et al., 2013). Nano-tube carbon deposition type were found in their catalyst after 50 h in reaction. It was very interest also that, the carbon was distinctly distributed at different position on the catalyst. Furthermore, the images also shows the carbon deposition was not encapsulating the active Ni particle. As a result, the deactivation of the catalyst derived from the active site coverage was effectively avoided.

2.2.2.2 Reverse water gas shift reaction

Water gas shift reaction is commonly found reaction associated with dry methane reforming. Methane reforming produces hydrogen and carbon monoxide. Reverse water gas shift reaction occurs when hydrogen and carbon dioxide exist in the system. Therefore, this side reaction is series reaction to dry methane reforming. Water gas shift reaction equation is given by:

$$CO_2 + H_2 \leftrightarrow CO + H_2O \qquad \Delta H_{298} = 41\ kJ\,mol^{-1} \qquad (2.15)$$

There are specific studies have been conducted by (Azzam et al., 2008) on water gas shift reaction of propane dry reforming. They found that, water gas shift reaction occur in two reaction routes either by redox or associative formate mechanism. Redox mechanism involves successive reduction and oxidation of the catalyst support while associative mechanism involves reaction an adsorbed surface intermediates. Water gas shift reaction strongly dependent on the type of catalyst support. Principally, this reaction is very significant in a system containing a rich amount of CO_2 and H_2. It is slightly endothermic and is likely to take place at a higher temperature than 1073 K. likewise, prompt removal of H_2 or CO_2 from the system would lower the contribution of the RWGS reaction.

2.3 Previous Study on various catalyst for methane dry reforming

This section is generally studying various type of catalyst used in methane dry reforming. This studies could be divided into some of the fresh catalyst characterization studies, dry reforming reaction activity ad carbon deposition study.

Table 2.2: BET specific surface area from previous study

Catalyst	specific surface area, m^2/g	Reference	Calcined temperature, K	Preparation method
Co-CeO_2	25	(Luisetto, Tuti, and Di 2012)	823	Co-Precipitation method
Ni-CeO_2	22			

Co-Ni/CeO_2	26			
14%Ni-Al_2O_3	209	(Castro Luna and Iriarte 2008)	1123	Sol gel
14%Ni-0.5%K-Al_2O_3	175			
14%Ni-0.5%Ca-Al_2O_3	192			
14%Ni-0.5%Mn-Al_2O_3	170			
14%Ni-0.5%Sn-Al_2O_3	179			
5% Ni/Al_2O_3	173	(Alipour, Rezaei, and Meshkani 2013)	773	Wet impregnation method
5% Ni-3% MgO/Al_2O_3	155			
5% Ni-3% CaO/Al_2O_3	154			
5% Ni-3% BaO/Al_2O_3	169			
P123/Ni-MgO	115.9	(Zanganeh, Rezaei, and Zamaniyan 2014)	873	Surfactant assisted co-precipitation
P123/Ni-MgO	100.3		973	
P123/Ni-MgO	49.81		1073	
19% Ni/MgO	32	(Frusteri et al. 2001)	673	incipient wetness
1%K-18.7%Ni/MgO	24			
3%K-17.3%Ni/MgO	21			
5%Ni/La_2O_3	15.2	(Ni et al. 2013)	1073	Co-precipitation
5%Ni/MgO-La_2O_3	8.8			
5%Ni/3MgO-La_2O_3	24.5			
5%Ni/5MgO-La_2O_3	20.6			
5%Ni/10MgO-La_2O_3	23.6			
5%Ni/20MgO-La_2O_3	30.3			
5% Ni/MgO	63.1			

Table 2.2 show BET specific surface area of some catalyst for methane dry reforming by different type of preparation method. Regarding to the table 2.2, Al_2O_3 utilization as catalyst support, increase the surface area as it is mesoporous surface and help the active metal Ni to disperse onto the catalyst surface. As aforementioned, carbon deposition

process favour acidic catalyst surfaces, thus additional alkaline earth metal could avoid the carbon formation onto the catalyst surface. Practically, it can be seen from the BET specific surface area of catalyst from previous study, addition of alkaline earth metal as promoter in some catalyst does reduce the specific surface area. Furthermore, the calcination temperature for the catalyst also does effect the specific surface area as can be seen from (Zanganeh et al., 2014) that study the calcination temperature effect on the specific surface area of P123/Ni-MgO catalyst. Different type of alkaline earth metal gives different surface area. (Ni et al. 2013) prepared 5%Ni/La_2O_3 and 5% Ni/MgO by co-precipitation method and the surface areas obtained is 15.2 m^2/g and 63.1 m^2/g. In this case, MgO as support gives more surface area compared to La_2O_3. Furthermore, (Zanganeh, Rezaei, and Zamaniyan, 2014) prepared Ni/MgO by surfactant assisted co-precipitation obtain the area is 115.9 m^2/g at 873K calcination temperature. Thus, in order to select the catalyst promoter and support, it must be in such way that it increases the specific surface area with basicity surfaces and calcined at the temperature that would not reduce the surface area of the catalyst significantly.

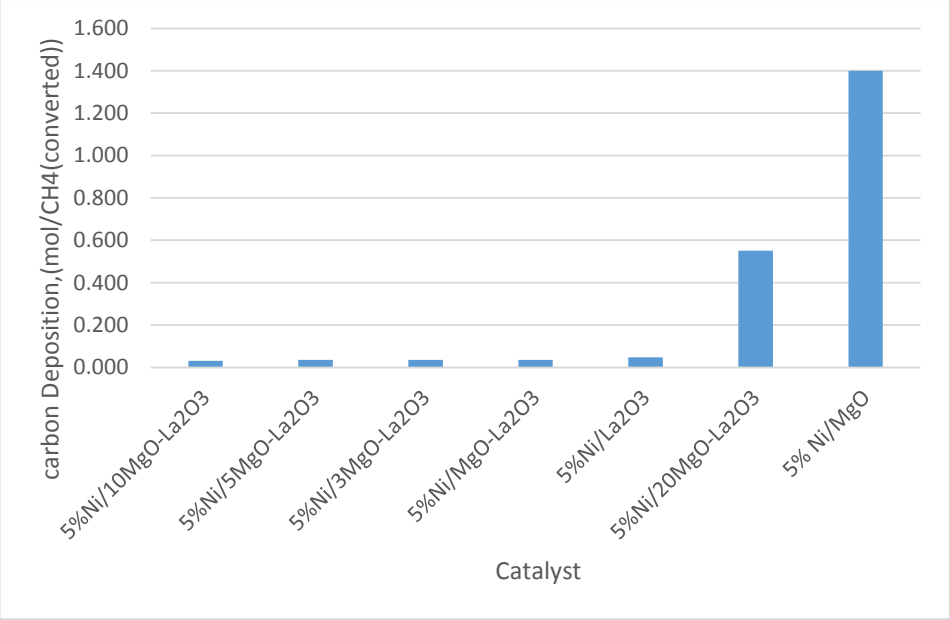

Figure 2.3: Carbon deposition on catalyst in methane dry reforming at 973 K with reactant volumetric flow CO_2/CH_4 at 1:1.

This study data were taken from (Ni et al., 2013) and plotted as a bar graph to see how the MgO as support and also as promoter affect onto the carbon deposition. Based on

the bar graph, the amount of carbon deposition can be arranged in a trend of 5%Ni/10MgO-La_2O_3<5%Ni/5MgO-La_2O_3<5%Ni/3MgO-La_2O_3<5%Ni/MgO-La_2O_3<5%Ni/La_2O_3 <5%Ni/20MgO-La_2O_3<5% Ni/MgO. Obviously the addition of La_2O_3 into Ni/MgO does help on reducing the carbon deposition. However, the addition of this La_2O_3 is giving reverse action toward methane conversion of 5%Ni/10MgO-La_2O_3 <5%Ni/5MgO-La_2O_3 <5%Ni/3MgO-La_2O_3 <5%Ni/MgO-La_2O_3 <5%Ni/La_2O_3 <5%Ni/20MgO-La_2O_3<5% Ni/MgO. Thus addition of La_2O_3 could benefit in avoiding the carbon deposition onto the catalyst but not to the methane conversion.

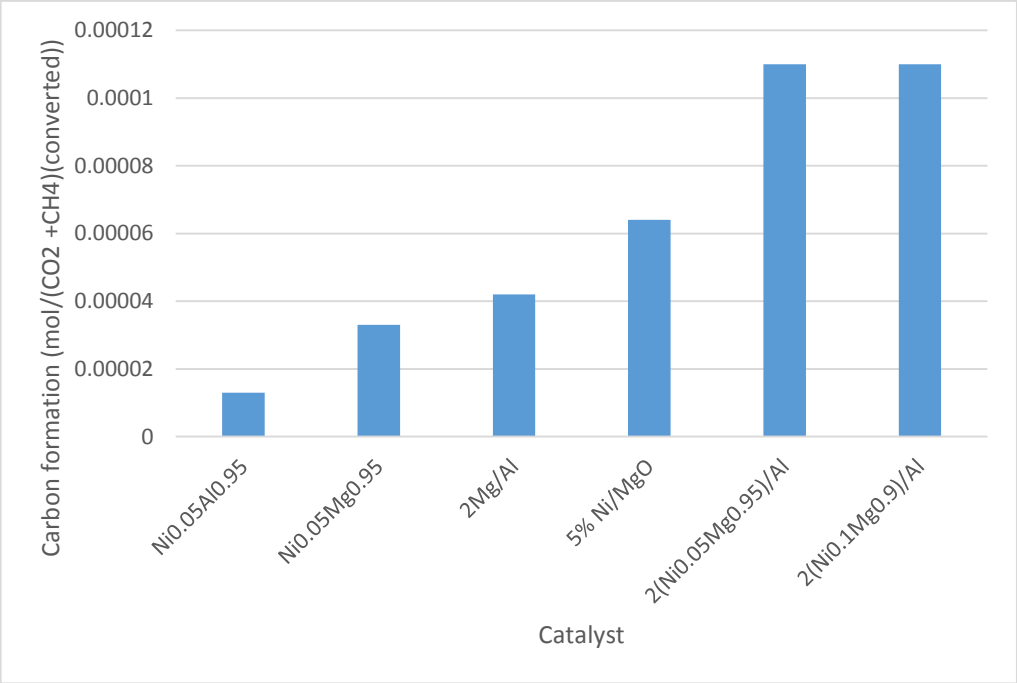

Figure 2.4: Carbon deposition per hour onto catalyst at 750 °C with volumetric CO_2/CH_4 ratio at 1:1.

Regarding to the bar plot above studied by (Djaidja et al., 2006), The addition of MgO as promoter into Al supported catalyst is not a good idea. The carbon deposition increases when MgO is added onto the catalyst with Al support. However, the carbon deposition on 5% Ni/MgO showing much lower than the $Ni_{0.05}Al_{0.95}$. This result might be due to the amount of Ni percentage in $Ni_{0.05}Al_{0.95}$ is lower compared to the 5% Ni/MgO as the carbon deposition sites is limited. However, to increase the product rates, the available actives sites of Ni must be atleast in the optimized amount. The methane conversion obtained using $Ni_{0.05}Al_{0.95}$ was 1.1% while 97.1% by 5% Ni/MgO. More catalyst weight is required to obtain the same conversion as 5% Ni/MgO in a

certain hour of reaction and hence increase the cost of catalyst usage in industry which is not practical even the carbon deposition rate is lower for $Ni_{0.05}Al_{0.95}$ compared to 5% Ni/MgO.

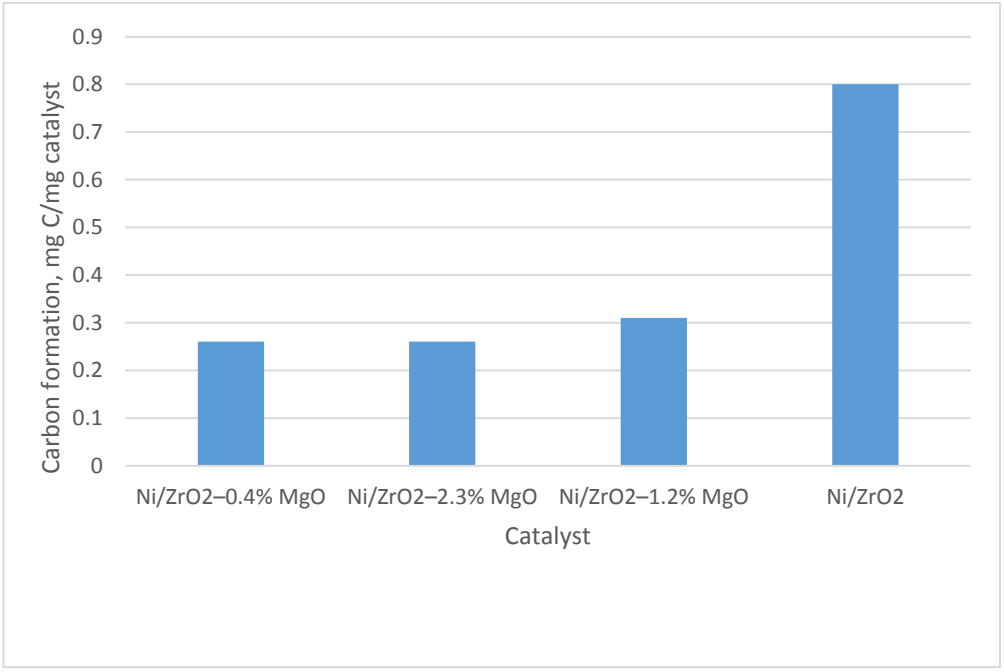

Figure 2.5: Carbon deposition onto catalyst at 873 K with CO_2/CH_4 volumetric ratio 1:1 after 5 hours in reaction.

Figure 2.5 also showing the carbon deposition onto the Ni-ZrO with MgO promoter(García et al., 2009). Based on the plot, addition MgO showing good result of reduced carbon deposition. Ni/ZrO alone without MgO promoter shows very high carbon deposition compared to the MgO promoted ZrO. Furthermore, it clearly shows the ZrO could not resist the carbon deposition unless promoted with MgO. MgO was found to inhibit the transformation of ZrO metastable phase to monoclinic phase and indirectly increase the thermal stability of the catalyst. Addition of Mg^{2+} and Ni^{2+} induced the reduction temperature to go higher.

Table 2.3: Reaction findings from previous study

Catalyst name	Reaction condition		Reference	Findings
	Temperature, K	CH_4:CO_2:Ar		
5% Ni/CZ/SBA-15 10% Ni/CZ/SBA-15 15% Ni/CZ/SBA-15 Ni/CZ/SBA-15 m.l Ni/SBA-15	873	1:1:8	(Albarazi et al., 2013)	1. Catalyst with 5 % Ni loading is the most stable catalyst. 2. Catalyst with 10 % loading shows highest conversion than the others. 3. Catalyst with 15 % Ni loading shows almost same conversion with 10% Ni loading shows almost same conversion as it has almost the same specific surface area. 4. Increasing amount of Ni% reduce the dispersion of Ni onto the catalyst surface and thus the surface area reduced.
Ni/Al Ni/SiAl Ni/MgAl Ni/ZrAl	923	1:1:0	(Damyanova et al., 2012)	1. Ni catalyst supported on MgAl having the best stability and high conversion on DRM as the Ni was disperse well with particle size of 5.1nm 2. Ni/SiAl found to have lowest methane conversion due to the agglomeration of Ni particle and filamentous carbon formation onto the catalyst.

Table 2.4: Reaction findings from previous study

Catalyst Name	Reaction condition		Reference	Findings
	Temperature, K	CH:CO2:Ar		
2Mg/Al $Ni_{0.05}Mg_{0.95}$ 5% Ni/MgO $Ni_{0.05}Al_{0.95}$ $2(Ni_{0.05}Mg_{0.95})/Al$ $2(Ni_{0.1}Mg_{0.95})/Al$	1023	1:1	(Djaidja et al., 2006)	1. $2(Ni_{0.1}Mg_{0.95})/Al$ gives the highest conversion with H_2/CO of 1.2 2. Calcination temperature of the catalyst at 873K, 1023K, 1173K for 2(Ni0.1Mg0.95)/Al does not affect the CH_4 conversion. However, it gives conversion in range of 97.1% - 97.6%. 3. 2(Ni0.1Mg0.95)/Al gives the lowest carbon deposition than other catalyst.
19% Ni/MgO 1.5%K-18.7Ni/MgO 2.5%K-17.3Ni/MgO	575-650 ^oC	1:1	(Frusteri et al., 2001)	1. Addition of K reduce the coking and sintering of Ni/MgO catalyst. 2. K addition increase the E_{app} 50kJ/mol to 70kJ/mol of the Ni/MgO by affecting the Ni electronic phase and supressed Boudouard reaction. 3. Addition more K into Ni/MgO, decreases the methane conversion. 4. Ni/MgO deactivation mostly due to the sintering and large amount of whisker carbon.

Table 2.5: Reaction findings from previous study

Catalyst Name	Reaction condition		Reference	Findings
	Temperature, K	CH:CO2:Ar		
5%Ni/MgO 5% Ni-0.1% Pt/MgO 5% Ni-0.3% Pt/MgO	973	1:1:0	(Meshkani & Rezaei, 2010)	1. All the prepared catalyst showing stable methane conversion for 50 hours. 2. Catalyst with lower Pt loading is showing higher conversion of methane compared to the catalyst that have higher Pt loading. 3. Pt could resist the carbon formation and hence increase the catalyst longevity.
10% Ni-5% Zr/SiO	873 923 973 1023 1073	1:1	(Yao et al., 2013)	1. Ni supported on SiO promoted by Mn shows better stability on stream than promoted by Zr. 2. At lower temperure of 1073 K, the catalyst stability reduced due to the ability of restraining the carbon deposition and exhibit good activity for reaction temperature of 873 – 1073 K. 3. Zr increase the reducibility of Ni-Zr/SiO and the catalyst deactivated much more dramatically as it could not resist carbon deposition.
10% Ni-5%Mn/SiO		1:1		

Table 2.6: Reaction findings from previous study

Catalyst Name	Reaction condition		Reference	Findings
	Temperature, K	CH_4:CO_2:Ar		
5% Ni/MgO 7% Ni/MgO 10% Ni/MgO 15% Ni/MgO	973	1:1:0	(Meshkani et al., 2013)	1. Ni catalyst with 5% Ni loading showing the most stable performance of DRM. 2. Ni catalyst with 15 % loading shows the highest methane conversion compared to the lower Ni loading catalyst.
NiO/MgO	1073	1:1	(Feng et al., 2013)	1. Calcination temperature study at 873 K and 1073 K was studies to test the catalytic performance on methane dry reforming. 2. NiO/MgO catalyst that calcined at 1073 K shows the best activity and metal support interaction. 3. Calcination of Ni/MgO at 1073 K, Ni^{2+} in the catalyst solid solution could help to have strong support interaction with support and resist coking.

Table 2.7: Reaction finding from previous journal

Catalyst Name	Reaction condition		Reference	Findings
	Temperature, K	CH_4:CO_2:Ar		
MgO 10%Ni/MgO 5%Ni-7%CeO_2/MgO 7% Ni-7%CeO_2/MgO 10%Ni-7%CeO_2/MgO 15%Ni-7%CeO_2/MgO	823-973	2:1	(Khajenoori et al., 2014)	1. 10%Ni-7%CeO_2/MgO shows the best activity in the Methane dry reforming. 2. The CO_2/CH_4 increase will reduce the coking formation on the catalyst. 3. Increasing the Ni percentage increase the particle size and indirectly reduces the Ni dispersion on the catalyst. 4. 10%Ni-7%CeO_2/MgO shows stable performance in reaction for 20 hours effectively.
$Ni_{0.03}Mg_{0.97}O$ $Ni_{0.07}Mg_{0.93}O$ $Ni_{0.10}Mg_{0.90}O$ $Ni_{0.15}Mg_{0.85}O$	823-973	1:1	(Zanganeh et al., 2013)	1. The increase in Ni content brought about a negative effect on the anti-coking performance in CO_2 reforming of methane on reduced solid solution catalysts. 2. A synergistic effect between high Ni dispersion and

$Ni_{0.25}Mg_{0.75}O$				basicity of support surface is suggested to produce very high resistance to carbon formation in CO_2 reforming of methane on reduced $Ni_{0.03}Mg_{0.97}O$ solid solution catalysts. 3. The formation of small Ni particles on the surface of the solid solution was attributed to the difficult reduction of NiO in the NiO-MgO solid solution catalysts.
Ni/Al_2O_3 $0.22K\text{-}Ni/Al_2O_3$ $0.18K\text{-}Ni/Al_2O_3$ $0.37K\text{-}Ni/Al_2O_3$ $0.49K\text{-}Ni/Al_2O_3$ $0.85K\text{-}Ni/Al_2O_3$ $1.26K\text{-}Ni/Al_2O_3$ $1.83K\text{-}Ni/Al_2O_3$ $5.00K\text{-}Ni/Al_2O_3$	973	1:1	(Juan-Juan et al., 2006)	1. The addition of potassium increases the reducibility of nickel species by hydrogen because it modifies the interaction of nickel oxide with the Al_2O_3 support. 2. Potassium migrates from the support to the Ni surface and neutralizes a fraction of the active sites. 3. Potassium catalyses the gasification of coke formed during reaction without modification of its structure. 4. Potassium does no modify the size nor the structure of the Ni particles.

CHAPTER 3

METHODOLOGY

3.0. Introduction

Basically this section will discuss in detail about the flow of the experimental work to accomplish this study with valuable result. The chemicals required, purity of the gas and the supplier is mentioned in this chapter. Additionally, equipment setting and fundamental theory of catalyst characterization equipment will be further detailed in this chapter.

3.1. Materials

Pr-Ni/MgO catalyst is being prepared in this particular study. Praseodymium nitrate hexahydrate, nickel nitrate hexahydrate and magnesium oxide are the chemicals which were bought is from Sigma-Aldrich Sdn Bhd and the product specification is detailed in Table 3.0:

Table 3.0: List of chemical for catalyst preparation

Chemical	Formula	Purity	Application
Praseodymium Nitrate	$(Pr(NO_3)_3).6H_2O$	> 98%	Catalyst preparation
Nickel Nitrate	$(Ni(NO_3)_2).6H_2O$	> 98%	
Magnesium oxide	MgO	> 98%	

The gases required for this study are carbon dioxide and methane as reactant for methane dry reforming. The purity of the gases are stated in Table 3.1:

Table 3.1: Gas required for reaction

Chemical	Formula	Purity	Application
Carbon Dioxide	CO_2	> 98%	Reactant Gas
Methane	CH_4	> 98%	

3.2 Catalyst Preparation

Pr-Ni/MgO was prepared by impregnation method. Both Pr and Ni salt solution were impregnated into MgO. Then, the catalyst was dried around 403 K for 3 hour. The dried catalyst was calcined at 1073 K for another 3 hours. Finally, the catalyst was prepared with desired size and shape for testing. The prepared catalyst contains 1-wt%, 3-wt% and 5-wt% of praseodymium. Figure 3.0 shows the process on the steps to prepare the catalyst by impregnation method.

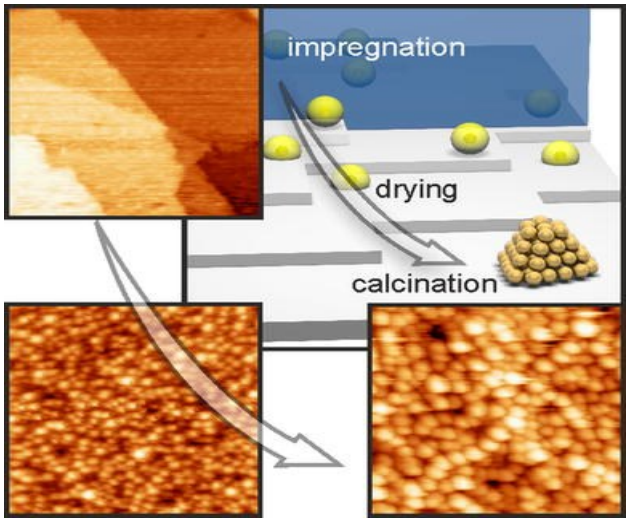

Figure 3.0: Image on catalyst preparation by impregnation method

Based on the Figure 3.0, the Pr and Ni were impregnated into MgO by the Pr nitrate solution and Ni nitrate solution. The amount of Pr nitrate solution requiredto obtain 1%, 3% and 5% Pr promoted was calculated and shown in appendix D. Then, it was mixed with 20 wt% Ni nitrate solution and further added with 80wt% of MgO. The impregnated catalyst solution was well stirred before it is dried. However, the drying catalyst was also being stirred for 30 minutes interval. The dried catalyst was calcined and broken into powder form and used for reaction test and characterization.

3.3 Catalyst Characterization

Physicochemical attributes give vital information about the physical and chemical features for characterized catalysts though N_2-physisorption (BET), X-ray photoelectron spectroscopy (XPS), Energy Dispersive X-ray Spectroscopy (EDX), X-ray diffraction (XRD), Field Emission Scanning Electron Microscopy (FESEM).

3.3.1 Brunauer- Emmett- Teller (BET)

Specific surface area of prepared catalyst is very important to predict the possible activity of the prepared catalyst. Of course there are many method employed to determine specific surface area of a catalyst. Currently, BET is the most common method used to determine the surface areas by adsorption and desorption with non-polar molecules such as nitrogen. This BET model is developed further from Langmuir theory (Langmuir, 1916). BET model equation is given by:

$$\frac{P}{V(P_o - P)} = \frac{(C-1)}{CV_m P_o} + \frac{1}{CV_m} \tag{3.1}$$

Where,

P is pressure of gas

V is the volume of gas adsorbed

$P_o$is the saturated vapor pressure of the liquid at the operating temperature

$V_m$is the volume of gas-adsorbed equivalent to monolayer coverage

C is a constant.

The plot of $P/(P_o - P)$V against the relative pressure P / P_oyields a linear relationship where Vm can be calculated from the slope and the intercept. The surface area then can be obtained from:

$$S_{BET} = \frac{V_m}{22414} \times 6.023 \times 10^{23} \times A_{N_2} \tag{3.2}$$

Where S_{BET} is the surface area per gram catalyst (m^2/g), $V_m$is the volume of the monolayer (mL) and the surface area of N_2 molecule, which is 16.2×10^{-20} m^2. In this study, multipoint BET surface areas for all the catalysts were obtained by N_2 adsorption at 77 K on surfer from Micromeritic, model ASAP2020

The procedure to conduct this test were as follows:

1. The sample about 0.25 g, was dried for 30 minutes at 298 K
2. Then, the sample degassed at 573 K for three hours and followed by cooling the sample at room temperature.
3. Subsequently, the sample tube was re-weighed to measure the real weight then transferred to the analysis station.
4. A Dewar flask filled with liquid $N_2$was placed in the holder underneath and N_2 level was checked with special thermostats that detect the level of coolant and accordingly move the Dewar up and down.
5. The adsorbed $N_2$was measured at different pressures and the values were then applied in Eq. 3.1 and *Vm* was obtained. This volume of the monolayer was then used in Eq. 3.2 and the surface area of the samples were calculated.

Determination of total pore volume and pore size distribution is the two common techniques that were used to describe porosity. For the evaluation of the porosity for most solid materials, N_2 at 77 K is the most suitable adsorbate (the material in the adsorbed state). The forces involved in Physisorption are the same as those responsible for the condensations of vapors, which include the London dispersion forces and the short-range intermolecular repulsion (Sing & Rouquerol, 1997). The pore volume is calculated at the P/P_o that close to the unity. The equation to determine the pore volume is given below:

$$V_{liq} = \frac{P_a V_{ads} V_m}{RT} \qquad (3.3)$$

Where,

V_{liq} is volume of N_2 liquid in pore

P_a is ambient pressure

V_{ads} is volume of gas adsorbed

R is gas constant

T is ambient temperature

3.3.2 X-ray Diffraction (XRD)

X-ray diffraction is practically used to measure the distance between two layers of atom and lattice phase of the catalyst. Electrons are produced from the heating tungsten that covered by cathode in a vacuum condition and accelerated towards the anode, which is at ground state. The high negative potential electron bombards the anode electrode (usually copper) and produces x-ray. Normally 1% of x-ray only being produced while the rest is dissipated as heat. This x-ray will passes through a window of beryllium that transparent to x-ray with measurable intensity and hit onto the sample (Norton, 1998). The resulting constructive interferences will be measured using the x-ray beam detector and become the fingerprint of the catalyst. The schematic diagram of XRD is shown is Figure 3.1:

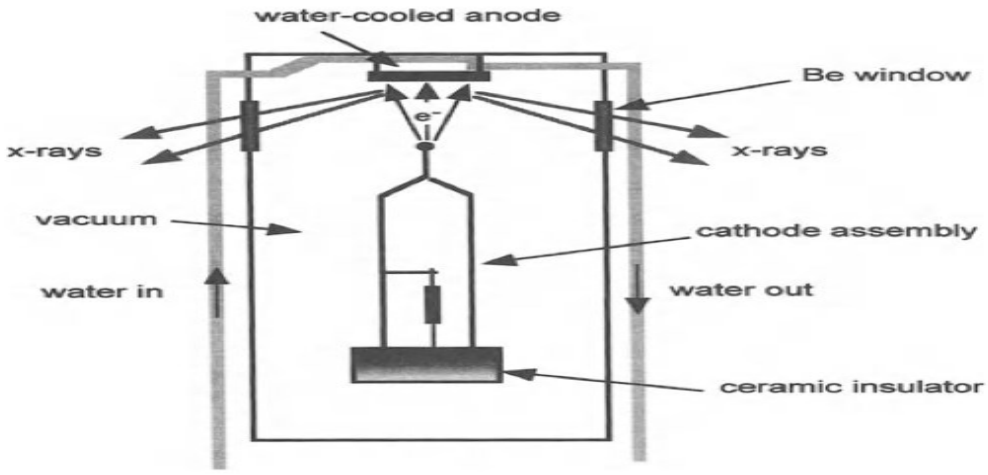

Figure 3.1: Schematic showing the essential component of X-ray tube.

Every component in the catalyst will show different peak at angle 2θ with known x-ray wavelength. Therefore, the distance in between two layers of atoms could be calculated using Bragg's equation (Cullity, 2001). Bragg's equation of distance between two layers of atom is given by

$$n\lambda = 2d\sin\theta \tag{3.4}$$

where n is the order of reflection (integer), λ is wavelength of x-ray beam (nm), d is inter plane distance of crystal (d-spacing) and θ is angle of incidence (degree). By

calculating the *d*-spacing of the catalyst, the phase can be determined by using this equation:

$$d_{hkl} = \frac{a}{\sqrt{h^2 + k^2 + l^2}} \tag{3.5}$$

Where, a is the length of cell edge and (*hkl*) is miller indices of the catalyst. The XRD measurements was carried out on RIGAKU, model of mini flex II system using CuK_α (λ = 1.542 Å) at 30 kV and 15 mA. The sample was blended to fine powder, to expose all the catalyst area as possible to obtain the spectrum at all angle. It is then placed on a glass specimen holder and pressed using a glass slide. The x-rays was first generated by a cathode ray tube, filtered to produce monochromatic radiation, collimated to concentrate and directed towards sample. The diffracted x-rays are then detected and the computer software plots a spectrum graph. The sample was scanned from 3° to 80° at a speed of 1° min^{-1}. The conversion of the diffraction peaks to *d*-spacing based on Diffraction Data (ICDD) database search match interpretation method allows the identification of the mineral since each mineral has a set of unique *d*-spacing.

3.3.3 Field Emission Scanning Electron Microscopy (FESEM)

Figure 3.2: Field Emission Scanning Electron Microscopy

Field emission scanning electron microscopy (FESEM) analysis can provide some information about catalyst surfaces morphology (size and shape) with three-

dimensional image. Moreover, SEM images can also abroad knowledge about the catalyst surface topography (surface features) and crystallography (atomic arrangement). All FESEM images obtained in this study were taken using a JEOL, model GSM 7800F at 10eV instrument which is fitted with secondary and backscatter electron detectors that allow for topographic and compositional (atomic number contrast) surface imaging of samples. This microscope will be able to magnify from ~10x to ~170,000x with images obtained up to 10 μm scale. The samples are coated with a thin layer of chromium to enhance conductivity and the instrument,was principally operated under high- vacuum mode to avoid conductivity problems. An electron gun is used to generate an electron beam that strikes the chromium-coated specimen to emit secondary and backscattered electrons. Image contrast is controlled in relation to the difference in the electron collection efficiency, which depends on the angle of emission, surface relief and atomic number of elements (Bergeret and Gallezot, 1997).

3.3.4 X-ray Photo-electron Spectroscopy (XPS)

X-ray Photoelectron Spectroscopy (XPS) is known, as Electron Spectroscopy for Chemical Analysis (ESCA) is a widely used technique to investigate the chemical composition of surfaces. It can be used to determine the composition in catalyst and the contamination exist in the catalyst before and after the catalyst spent. X-ray is being used to knock out the electron in the atoms. These electrons allow us to measure the binding energy of that particular catalyst atom and show us how strong are the electrons bonded toward photon. This information indirectly enable us to determine the element exist in the catalyst referring to their bond energy. XPS will be carried out on a JPS-9010 instrument to investigate the composition of deposited films by ionizing surface atoms and measuring the energy of ejected photoelectrons. La-Ni/MgO catalyst specimen (in spherical form) will be bombarded with low energy X-rays source of Al Kα (1486.3 eV). The X-rays caused photoelectrons with binding energy, E_b, to be ejected from either valence or inner core electron shell when an atom absorbed a photon of energy, hν. The kinetic energy of the photoelectron, E_k, given by Equation (3.6)

$$E_k = h\nu - E_b - \Phi \qquad (3.6)$$

where, *h* is the Planck's constant, *v* is frequency of the exciting radiation, E_b is the binding energy of the photoelectron with respect to the Fermi level of the sample and Φis the work function of the spectrometer. In order to avoid contamination, the analysis is carried out at ultra-low vacuum pressure ($<10^{-10}$ mbar).

3.3.5 Energy Dispersive X-ray (EDX)

EDX is a quantities and qualitative measuring equipment. It can be used to measure the amount of certain component in the catalyst and the type of components exists in the catalyst. Since the EDX is measured from the binding energy of the atoms. Therefore, the incoming electron beam must have high energy that more that the binding energy of the sample atom to knock out the electrons. The detection schematic diagram is shown in figure 3.3

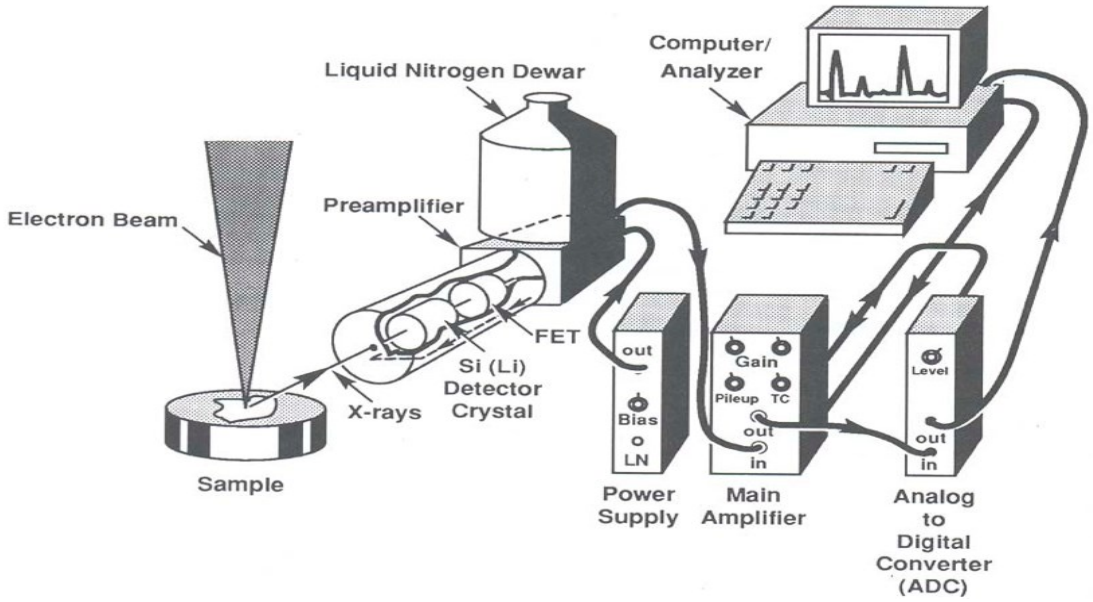

Figure 3.3: Schematic representation of energy dispersive x-ray spectrometer

When the detection crystal captures x-ray photons they create electron-hole pairs. These electron-hole pairs are formed charge pulse by the applied bias and they are further converted to voltage pulse by a charge-to-voltage converter. The signals further amplified and shaped by a linear amplifier and finally passed to a computer x-ray analyser (CXA), where the data is displayed as a histogram of intensity by voltage

(energy).The key to understand how an energy-dispersive X-ray spectrometer (EDS) works is to recognize that each voltage pulse is proportional to the energy of the incoming x-ray photon.

3.4 Experimental Apparatus

Prepared catalyst was tested in a fixed-bed reactor. Around 0.3 g of catalyst was placed onto quartz wool in the fixed bed reactor with internal diameter of 10 mm. Two layer of quartz glass wool supports the catalyst. The catalyst was purged with H_2/Ar gas for 2h at 50 ml min^{-1} STP at 973 K to reduce the catalyst. The $CH_4$and $CO_2$was controlled with adjustable flow meter. The syngas produced was taken at interval of 15 minutes, 60 minutes and 120 minutes and tested by using chromatography provided in laboratory of University Malaysia Pahang. The apparatus diagram is shown in figure 3.4:

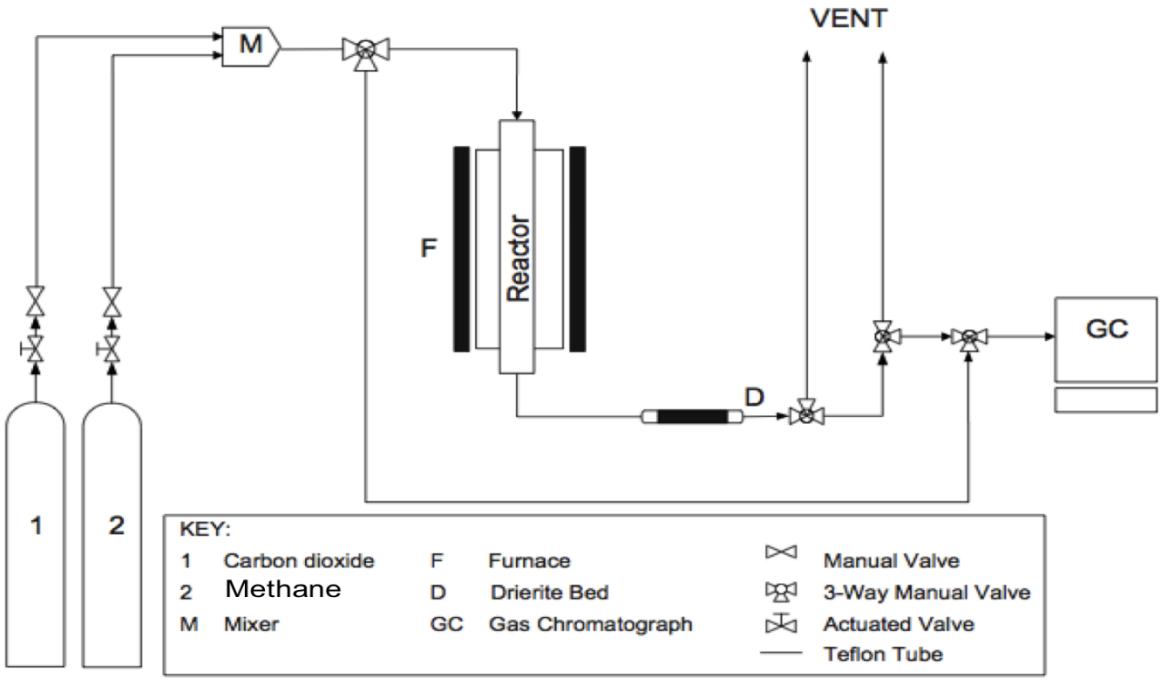

Figure 3.4: Experimental set up apparatus for methane dry reforming

Catalyst prepared contains 0 %wt, 1 %wt, 3 %wt and 5 %wt of promoted praseodymium were tested in this particular methane dry reforming. Every catalyst prepared were tested at temperature 1073 K, 1123K and 1173Kat flow ratio of 1:1 for CO_2:CH_4 in order to determine the methane conversion and carbon dioxide conversion.

The gaseous sample was collected into a tedlar sampling bag and send to lab of University Malaysia Pahang for composition test. Once the analysis on the composition is completed. The methane and carbon dioxide formation with respective Pr loading percentage is plotted and observed. The best praseodymium loading is selected based on the amount of conversion of methane and carbon dioxide. Then that catalyst is selected for further test to observe on the conversion of the catalyst. The selected parameter for this further test is reactant volumetric flow ratio. (Tottrup, 1976) stated that carbon monoxide decomposition rate decreases when the amount of carbon dioxide increases at temperature above 573 K. Therefore, ratio of CO_2: CH_4 in this study decided is 1:9, 1:4, 1:1, 4:1 and 9:1 is selected for further investigation.

CHAPTER 4

RESULT AND DISCUSSION

4.1 Fresh Catalyst Characterization

4.1.1 Liquid N_2 Physisorption

The physical properties of Pr – Ni/MgO obtained from this test is BET specific surface area, and pore diameter. Figures 4.1 and 4.2 show the samples of BET isotherm pattern for the 1 % promoted Pr and 5 % promoted Pr.

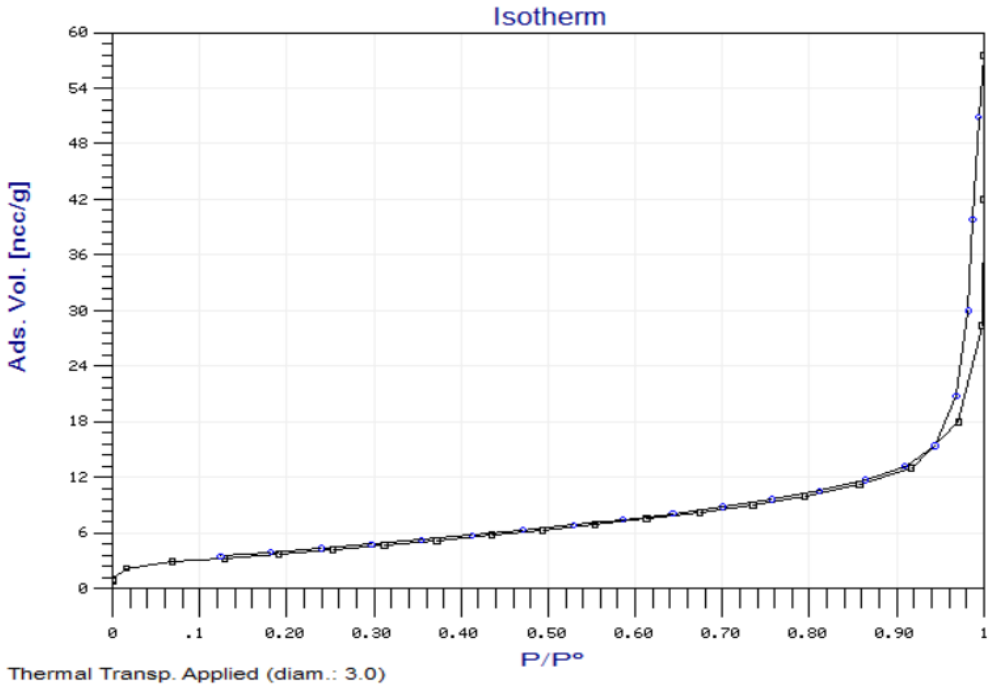

Figure 4.1: BET isotherm plot of 1% Pr of Pr-Ni/MgO

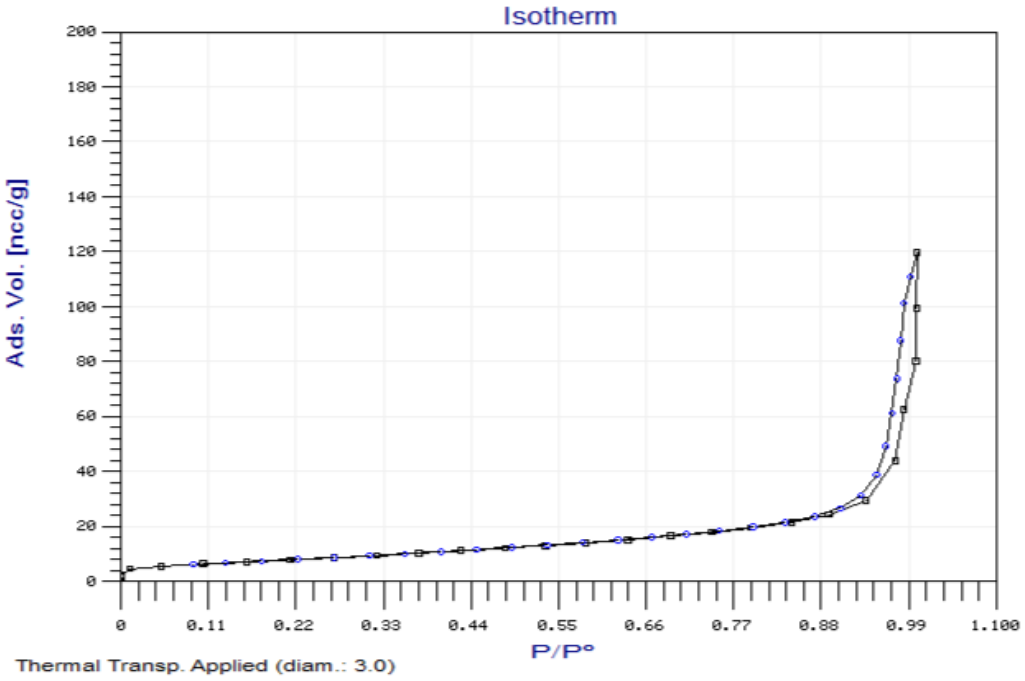

Figure 4.2: BET isotherm plot of 5% Pr of Pr-Ni/MgO

Table 4.1 shows the BET specific surface area of Ni/MgO catalyst increased upon Ni-impregnation and further increased once Pr was promoted. Furthermore, the addition of promoter over Ni/MgO showed direct correlation, which means the BET specific surface area increased as the amount of promoter increased. However, the pore diameter of this microporous catalyst showed the addition of Ni into MgO increased the pore diameter. As it can be seen, the pore diameter of MgO alone was 0.94 nm and the addition of Ni increased the pore diameter to 0.97 nm. When the addition of just 1% Pr into Ni/MgO the pore diameter reduced from 0.97nm to 0.87nm. The pore diameter, reduced further into 0.80 nm when the addition of 5% of Pr into Ni/MgO. Significantly, this is symptomatic of pore plugging

Table 4.1: BET specific surface area, Pore volume and pore diameter

Sample catalyst	BET surface area, m^2/g	Pore Diameter, nm
1% Pr-20% Ni/MgO	14.30	0.87
5% Pr-20% Ni/MgO	28.11	0.80
MgO	8.51	0.94
20% Ni/MgO	14.04	0.97

4.1.2 FESEM Imaging

The images of fresh catalyst were taken using FESEM to study the structure of the catalyst. The images in figures 4.3 and 4.4 show the structure of the Ni/MgO and 5% Pr-Ni/MgO.

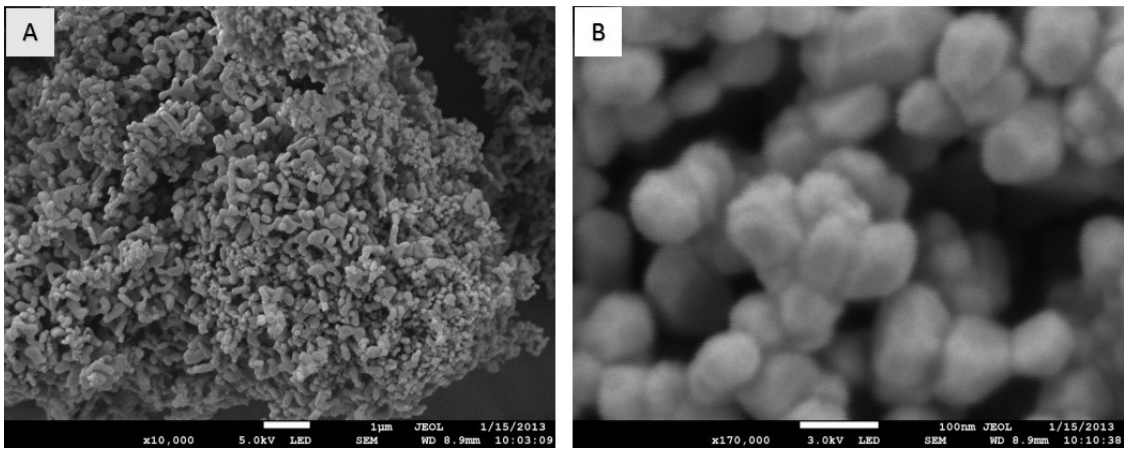

Figure 4.3 Ni/MgO fresh catalyst FESEM images at 10k and 170k

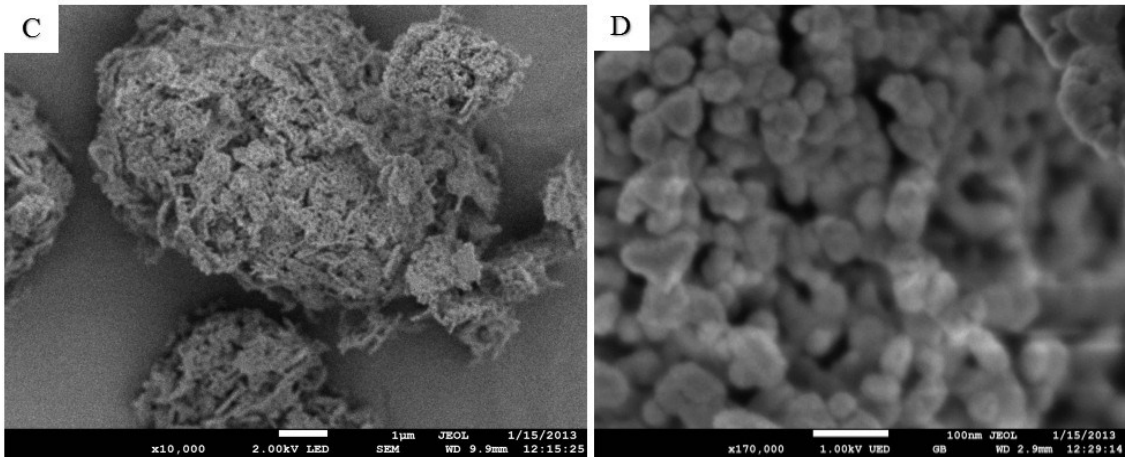

Figure 4.4: 5% Pr-Ni/MgO Fresh catalyst FESEM image at 10k and 170k

Based on the image, the Ni/MgO alone does not closely packed structure (Image 4.3B); however, after 5% Pr was promoted into Ni/MgO the structure was more closely packed compared to Ni/MgO alone as suggested by both Images 4.4C and 4.4D. Obviously, the structure looks less porous when Pr was added due to smaller particle diameter. This observation has explained the decrease in pore volume of the Ni/MgO upon Pr promoter inclusion.

4.1.3 X-ray Diffraction

Figure 4.5 shows the x-ray diffraction pattern of the 5% Pr-Ni/MgO catalyst. There were no PrO peak found as it was finely dispersed onto support.

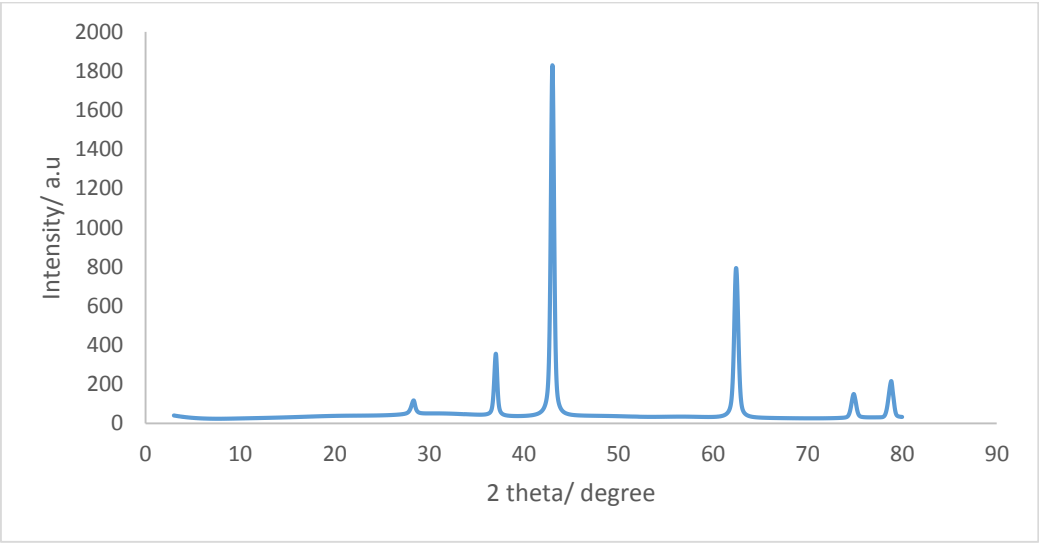

Figure 4.5: X-ray diffraction pattern of 5% Pr promoted Pr-Ni/MgO

(Meshkani & Rezaei, 2011) studied the XRD pattern on the Ni/MgO with various nickel loading shown in Figure 4.6.

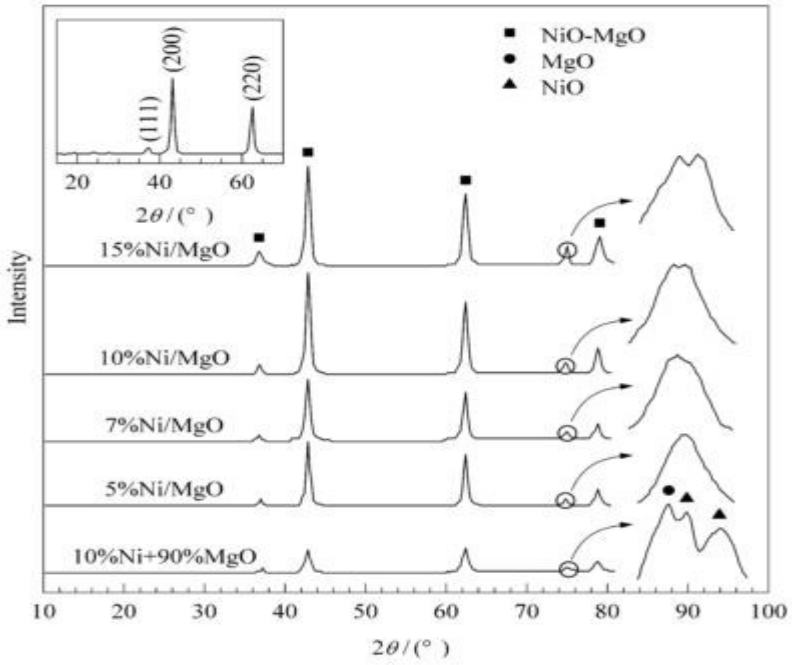

Figure 4.6: XRD pattern of Ni/MgO of various Ni loading.

Regarding to Figure 4.6, the intensity peak at 2-theta range of 70^{o}-80^{o}, shows two peak assigned as MgO and NiO for 15%Ni/MgO and 10%Ni/MgO. The 7% Ni/MgO and 5% Ni/MgO seem to have only a peak. This indicates that, the NiO and MgO are incorporated become NiO-MgO solid solution. It can be concluded that, the Ni loading more than 7% does not result into much NiO-MgO solid solution in the catalyst. For this study the 5%Pr-20%Ni/MgO shows only a peak at the angle 2 theta range of 70^{o} – 80^{o} shown in Figure 4.7.

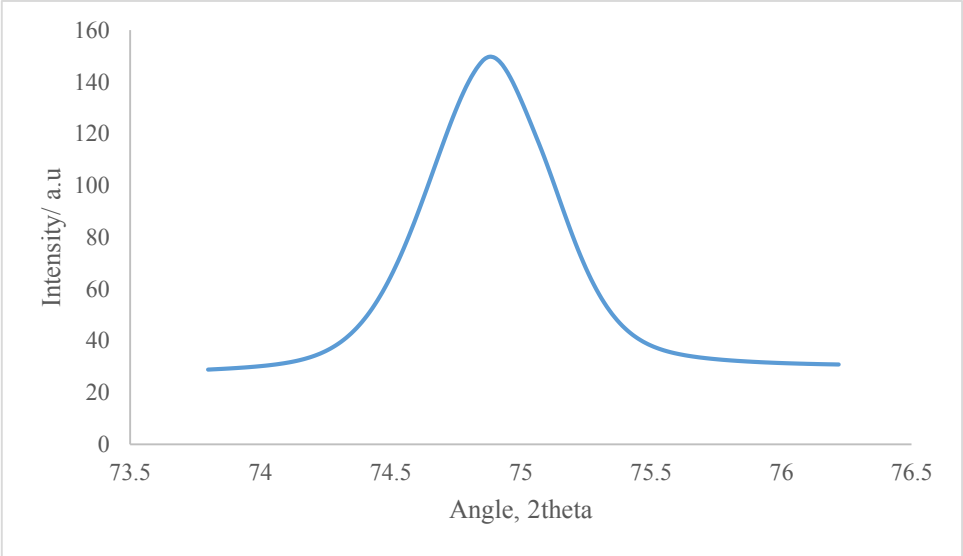

Figure 4.7: Intensity peak at 70º-80º

(Meshkani & Rezaei, 2011) stated that, the incorporation of NiO-MgO into solid solution is depending on the Ni percentage in the Ni/MgO and the calcination temperature. Promotion of Pr into 20% Ni/MgO seems to help the Ni to be well incorporated with MgO compared to Ni/MgO alone with nickel loading more than 7% based on (Meshkani & Rezaei, 2011) study. There were no PrO peak found in the 5% Pr-Ni/MgO. The peak 2- theta for NiO-MgO can be seen at 28.339, 37.022, 42.994, 62.994, 62.404, 74.85, and 78.83. The highest intensity peak was found at 42.994 which indicate that, the Pr-Ni/MgO has very good crystallinity.

4.1.4 Energy Dispersive X-ray Spectroscopy (EDX)

EDX was used to obtain the type of element contained in specific catalyst and the amount of those elements. The resulting EDX profile for 5 % Pr is shown in Figure 4.8 as representative of solid catalyst sample.

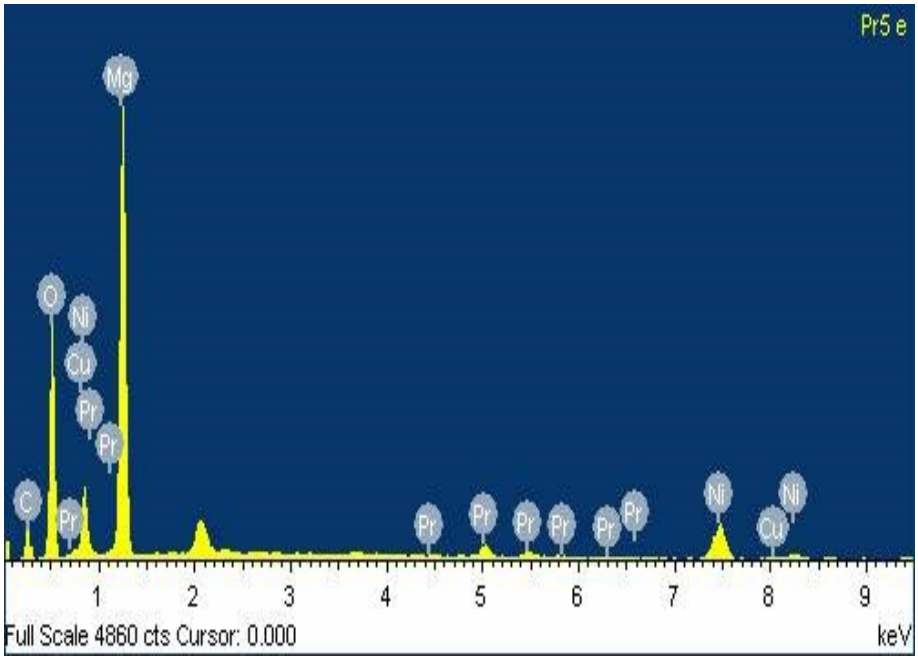

Figure 4.8: EDX profile of 5% Pr loading of Pr-Ni/MgO

From the profile and the resulting element analysis provided by the instrument, the data shows that there were 18.37% Ni and 5.07% Pr contained in the catalyst. Therefore, this catalyst was used in the reaction study as it correct amount of promoter for this study scope. The element Mg and oxygen was contributed from the MgO itself. The Detailed element and amount is attached in appendix A.

4.2 Dry Reforming Reaction Studies

4.2.1 Catalysts Screening and Temperature Parameter Selection

Catalyst screening was conducted to select the best performing catalystfor further testing. Furthermore, the best temperature of the reaction was chosen within this screening process. Thus all catalyst was subjected to:

1. The temperature parameter effect on rate of H_2 and CO formation.
2. The temperature parameter effect on the conversion.
3. The temperature effect on the Product ratio of H_2/CO.

This screening was conducted at CO_2 and CH_4 volumetric flow ratio of unity. Once the best amount of Pr promoted catalyst was selected, further testing parameter were conducted for that selected catalyst.

4.2.1.1 Temperature Effect on Rate of Formation

Figure 4.9 shows the rate of H_2 formation at three different temperature of 1073K, 1123K and 1173K respectively. Overall observation shows the rate of H_2 formation rates were directly proportional to the temperature. This is consistent with Arrhenius equation as higher temperatures would increase the reaction rate.

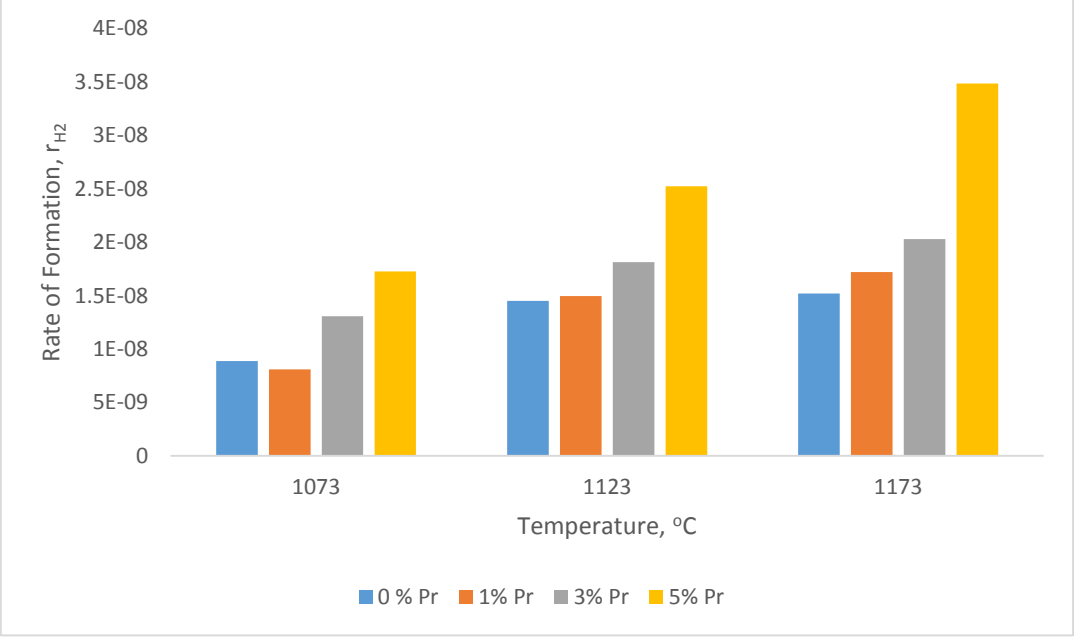

Figure 4.9: Rate of H_2 formation over temperature

Moreover, it can be seen that across the different temperatures, unpromoted Ni/MgO showed the slowest H_2 formation rates that incrementally increase with the amount of Pr-metal loading. Overall, H_2 formation rate increased in the sequence of 0wt% Pr < 1wt% Pr < 3 wt% Pr < 5 wt% Pr. The slight increase recorded for 1wt% Pr compared to the unpromoted Pr can be assigned to the BET specific surface area result of both catalysts. The area per gram for the 0% and 1 % promoted Pr was 14.01 m^2/g and 14.30 m^2/g respectively which indicates slight improvement. Since the Ni weight percentage formulation was similar for both 1% and 0% Pr promoted Pr-Ni/MgO catalysts, therefore, it can be concluded that, the 1% Pr addition possessed higher BET specific surface area for greater accessibility for reactants. Significantly, when the amount of Pr-metal increased, the H_2 formation rate also substantially-increased. This could be that the Pr promoted the well dispersion of Ni metal on the surface of support and consequently the active metal site also would increase. Regarding to the graph, 5% Pr promoted Pr-Ni/MgO shows the highest rate of H_2 formation of all the other amount of the promoted catalyst. Furthermore, the catalyst specific surface area for 5% Pr/Ni/MgO was the highest among the 0%, 1%, 3% Pr promoted catalyst. Figure 4.10 show the trend of the amount of Pr promotion of to the product ratio H_2/CO.

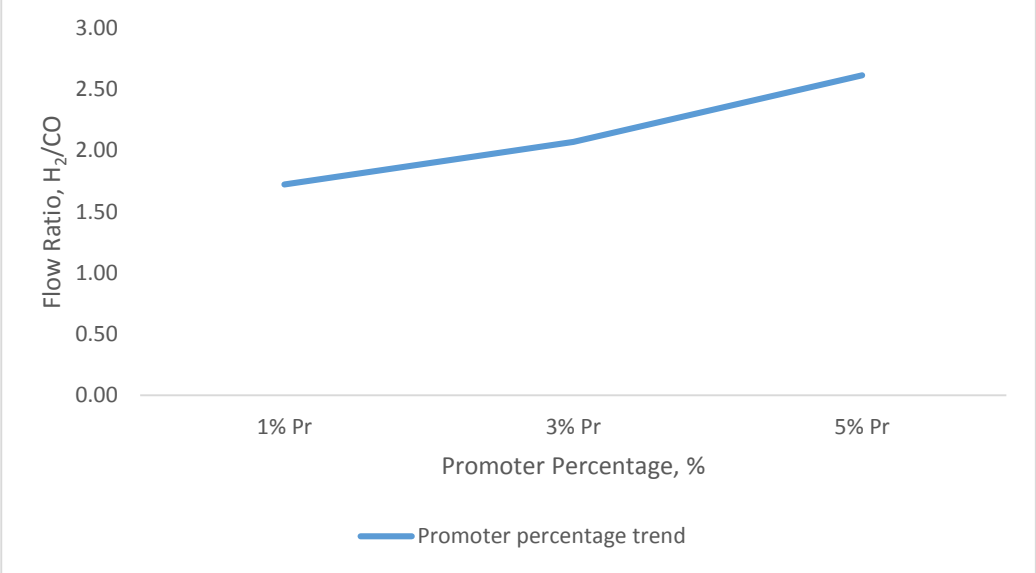

Figure 4.10: Effect of promoter percentage to the product ratio of H_2/CO at 900 °C and 1:1 reactant volumetric flow ratio

Based on this graph trend, the amount of Pr promotion increases the product ratio. Furthermore, the product ratio does not exceed 3 for all the amount of promotion which was consistent with earlier studies, for example report by (Özdemir et al., 2014).In their paper entitled 'CO_2 reforming of methane over nickel catalysts supported on nanocrystalline $MgAl_2O_4$ with high surface area',it was shown that the product ratio H_2/CO never exceed 3. The level of Pr promotion has increased the H_2/CO composition ratio of the product.

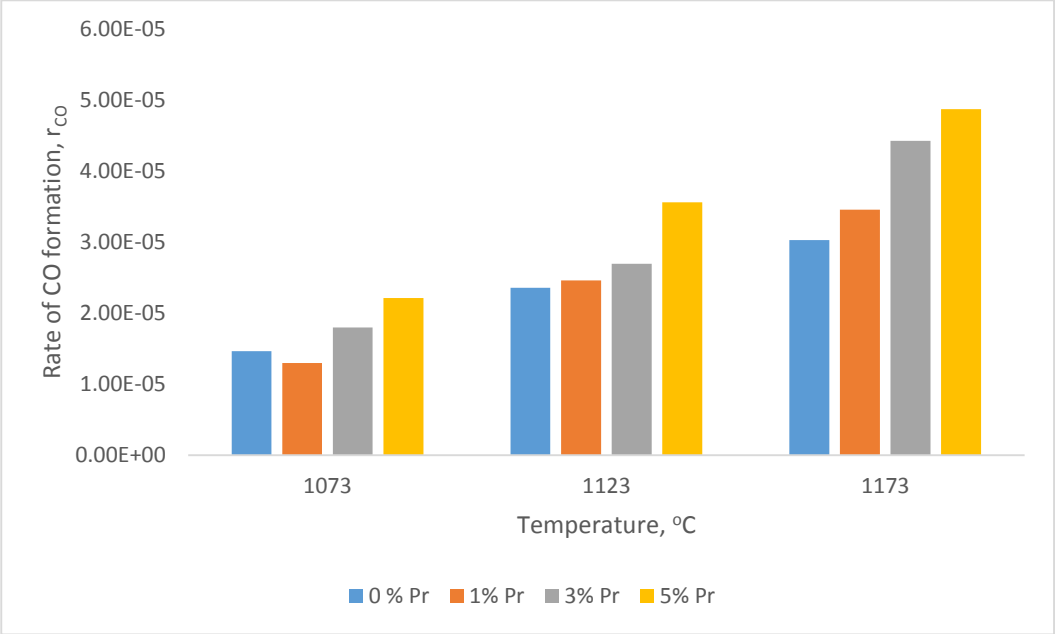

Figure 4.11: Rate of CO formation over temperature

Figure 4.11 shows the rate of CO formation at various temperature. The graph show the same positive trend of temperature to rate of CO formation. The CO formation also increased when the temperature increased. The 5% Pr promoted catalyst showed highest rate of CO formation at all temperatures compared to the other catalysts. However, Comparing figure 4.9 and figure 4.11, the rate of formation for CO was larger than H_2 of all catalyst and at all temperature. This may be due to the fact that the carbon source is readily available from both CH_4 and CO_2whilst the H_2 is only available from CH_4. Furthermore, the high CO formation rate also could be the concluded that the carbon deposition was suppressed over the catalyst as Pr which is the electron promoter that will reduce the coke formation on the catalyst.

4.2.1.2 Temperature Effect on Methane Conversion

Figure 4.12 shows the temperature effect on methane conversion with different amount of promoted Pr. The conversion of 1% and 0% promoted Pr shows almost the same conversion at all different temperature. It also already shown from the result of rate of formation of H_2 that factor to the amount of the conversion of methane on those particular catalyst and thus gives almost the same conversion for both 0% and 1% Pr promoted catalyst. The methane conversion obtained from the 5% Pr at 900 ^oC was 61.4%. The 3 % Pr promoted conversion was 40.34% and 1% and 0% Pr promoted was 23.63% and 23.31%. Among these catalyst, 5% does gave high methane conversion that the others. Therefore, the 5% Pr promoted Pr-Ni/MgO having the high chance to be selected. However, the other data also was compared to have a concrete reason to select it.

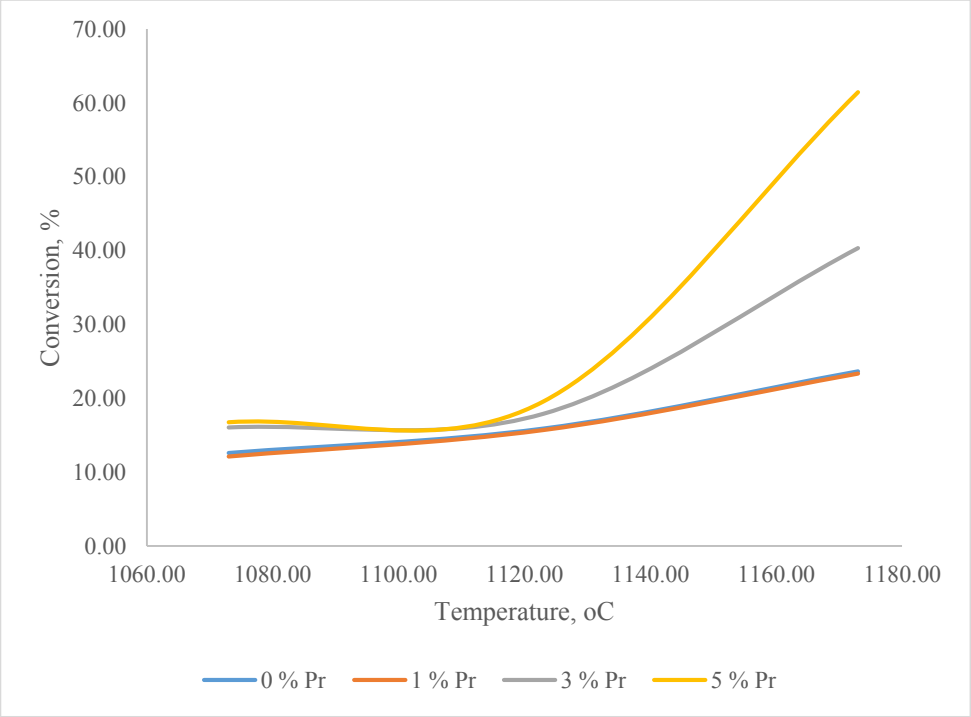

Figure 4.12: Temperature effect on conversion of 0% Pr, 1% Pr, 3% Pr, and 5% Pr promoted in Pr-Ni/MgO.

4.2.1.3 Temperature effect on product ratio of H_2/CO

Figure 4.13 shows the product H_2/CO ratio over temperature of 0%, 1%, 3% and 5% Pr loading in Pr-Ni/MgO catalyst. The temperature of the reaction is linearly related to the product H_2/CO ratio. At lower temperature, the product H_2/CO ratio is lower and get higher at high temperature. The interesting result obtained on this data is the H_2/CO composition ratio, which shows low enough as it is very suitable for Fisher-Tropsch synthesis (Ruckenstein & Hu, 1996) Among those all catalyst tested, the 5% Pr promoted Pr-Ni/MgO is selected for reactant flow ratio effect at 900 °C as this temperature gives the most significant rate of formation for both H_2 and CO, High conversion, and high product H_2/CO ratio.

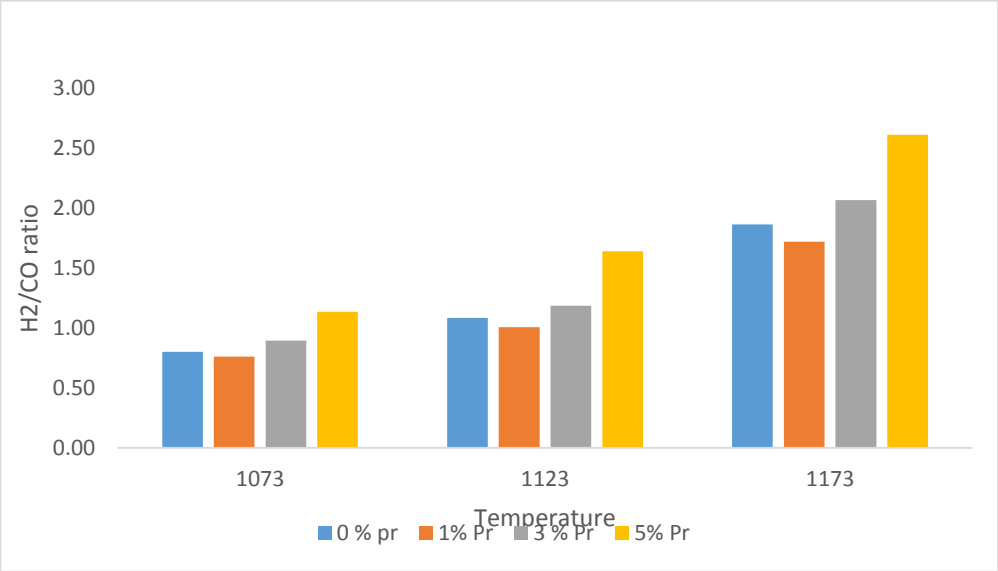

Figure 4.13: Temperature effect on the product ratio of H_2/CO

4.2.2 The Reactant CO_2/CH_4 Flow Ratio Effect on 5% Pr of Pr-Ni/MgO

Figure 4.14, shows the effect of CO_2/CH_4 Reactant volumetric flow ratio effect on the rate of H_2 and CO formation. The trend of H_2 formation is decreasing as the reactant CO_2/CH_4 increasing. As the ratio increase, its means that the amount of CH_4 in the inlet is lower compared to CO_2. Therefore, the rate of H_2 formation decreases due to the CH_4 is the source of the H_2 formation. However, the trend shown by CO formation is increasing until the CO_2/CH_4 ratio is 1:4 and reduces as the ratio increase more than 1:4.

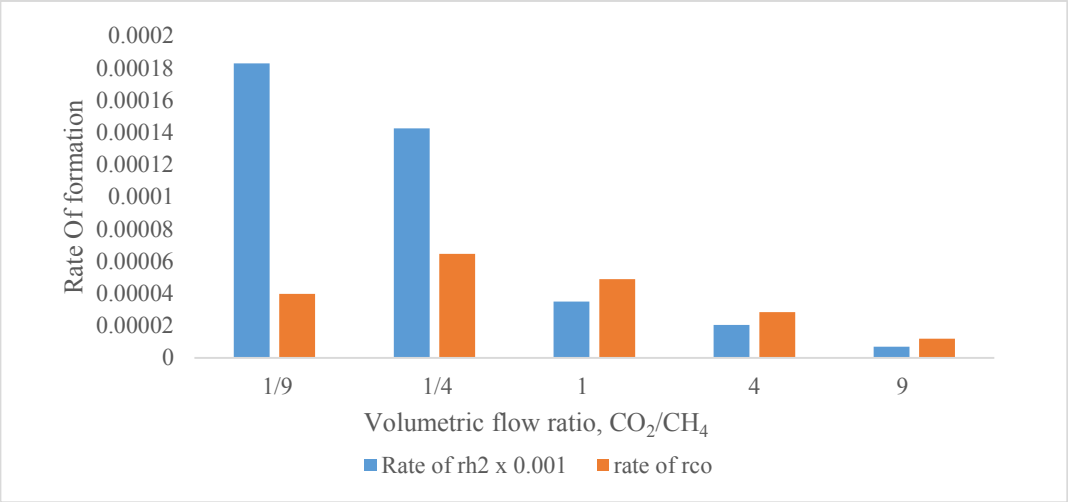

Figure 4.14: Rate of H_2 and CO formation effect by various reactant flow ratio CO_2/CH_4 at 900ºC.

Based on figure 4.15, the reactant flow ratio CO_2/CH_4 effect on the conversion for 5% Pr-Ni/MgO catalyst. The trend showing that, there is an optimum ratio that allow this catalyst to obtain high conversion. It can be seen that, the conversion at CO_2/CH_4 ratio of 1:1 is the highest. As the CO_2/CH_4 ratio reduces, it means there are more CH_4 than CO_2 in the inlet flow. The conversion reduces when more CH_4 is used than CO_2. This situation could be due to the rate of carbon deposition is higher when the reactant CO_2/CH_4 is lower than the optimum. This statement supported by (Tottrup, 1976) which in his study states the increasing amount of CO_2 could reduce the carbon deposition rate on the catalyst.

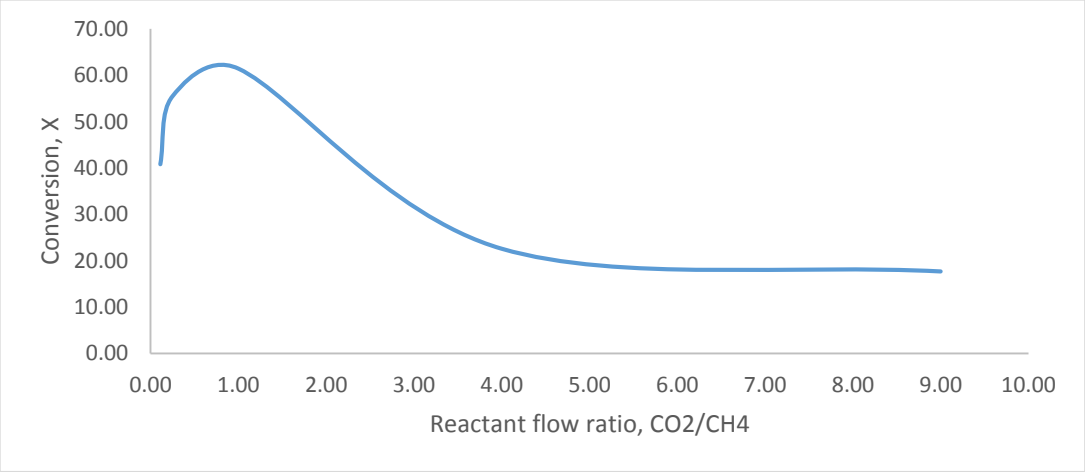

Figure 4.15: Effect of reactant flow ratio on the CH_4 conversion for 5% Pr at 900 ºC

4.3 Determining the Rate Law

Rate law is the most important equation which represent the overall scene of methane dry reforming reaction. The rate law was determined from experimental work. The reactant concentration order is determined first and then the reaction rate constant, k. Initial rate method is used to determine the concentration power order. The power order obtained from the calculation is 0.6111 for CH_4 and 0.42741 for CO_2. The reaction rate constant is determined from the data which the reactant concentration is set constant and the temperature is varied, and a graph of ln k versus 1/T is constructed. The graph of ln k versus 1/T is shown in figure 4.16.

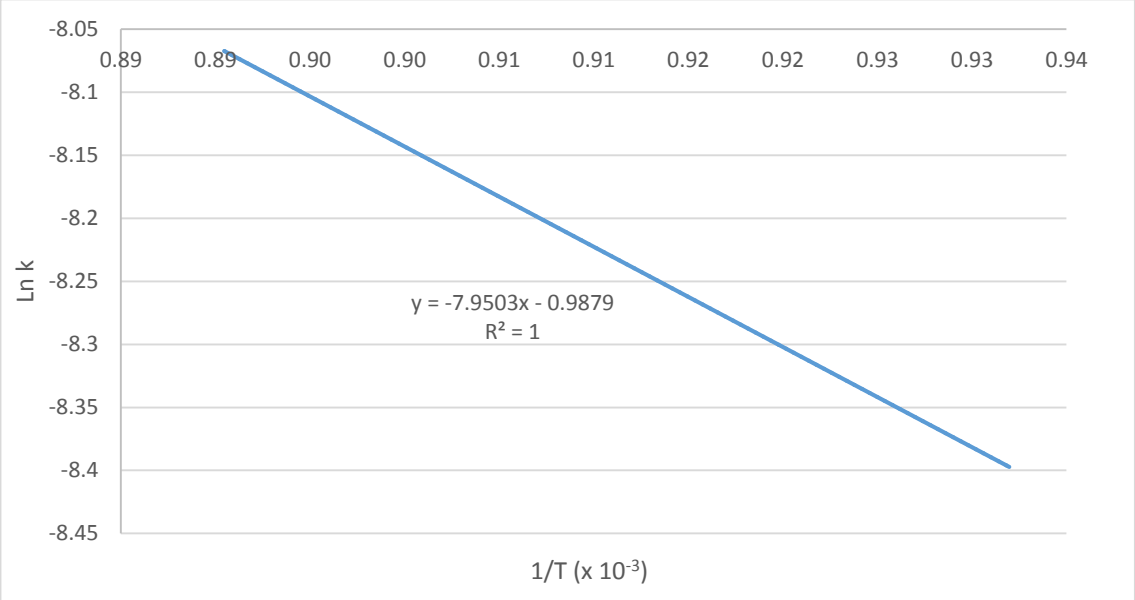

Figure 4.16: ln k versus 1/T

The gradient is representing the $-E_a/R$ and the intercept is ln A. Activation energy calculated from this graph is 66.098 kJ/mol and the activity, A is 0.372. The overall rate law obtained is given by,

$$-r_{CH_4} = k\left[CH_{CH_4}\right]^{0.6111}\left[CO_2\right]^{0.42741}$$

Where, $k = 0.372e^{-66.098/RT}$ valid in temperature range of 1072K-1173K

Based on the activation energy found on this reaction respect to CH_4, it higher compared to Ni/MgO calculated by (Frusteri et al., 2001) at 50 kJ/mol. Furthermore, in this article does mention that, changes in E_a is due to the alkaline promoter which induced electron enrichment onto the active sites of Ni and hence supress the carbon deposition on the catalyst. Thus, the increment in the E_a of the 5%Pr-Ni/MgO to 66.098 kJ/mol must be due to the Pr addition onto the catalyst.

CHAPTER 5

CONCLUSION AND RECOMMENDATION

5.1 Conclusions

Based on the study conducted in this thesis, several matters could be outlined are BET result showing increase in specific surface area on Ni/MgO after Pr promotion in the sequence of 5%Pr-Ni/MgO>3%Pr-Ni/MgO>Ni/MgO>MgO. The surface area exhibit by Ni/MgO and 1% Pr-Ni/MgO shows almost similar. Pore diameter shows negative sequence such that the increment of Pr promotion reduces the pore diameter. XRD pattern shows no peak found for the PrO and almost all peak represent NiO-MgO. It was showing that the interaction of the PrO and NiO with the MgO is strong enough. The peak of NiO-MgO was found at angle 2theta of 28.339, 37.022, 42.994, 62.994, 62.404, 74.85, and 78.83. Furthermore, EDX result also showed that the percentage amount of Ni and Pr in the catalyst was 18.37% and 5.07 % for the 5% Pr promoted catalyst suggesting that catalyst preparation method was valid. FESEM images for fresh 5% Pr-promoted catalyst was much closely packed than the unpromoted Ni/MgO which was consistent with the BET result on the pore diameter which were reducing as Pr promotion increases. The reaction studies conducted over the prepared catalyst of 1%, 3% and 5% Pr and screened to obtain the best catalyst for CO_2/CH_4 reactant volumetric flow ratio study. Reaction study was conducted at 1073K, 1123K and 1173K with reactant CO_2/CH_4volumetric flow ratio of 1:1. Overall reaction studies found was the 1%Pr-Ni/MgO and Ni/MgO catalyst shows the same rate of H_2 and CO formation at all tested temperature. Thus the addition of 1% Pr-Ni/MgO catalyst was not significant compared to 3% and 5% Pr-Ni/MgO. The 5% Pr-Ni/MgO highest rate of H_2 and CO formation compared to the other catalyst. The H_2/CO ratio obtained for all catalyst on methane dry reforming was less than 3 at reaction temperature ranged 1073K – 1173K with reactant CO_2/CH_4volumetric flow ratio of 1:1. The Pr addition percentage on Ni/MgO shows linear relation to the H_2/CO composition ratio. As the Pr promotion

percentage increases, the H_2/CO ratio increases. 5% Pr-Ni/MgO exhibit the best activity on the methane dry reforming than the other catalyst. The 5% Pr catalyst tested at 1173K with CO_2/CH_4 volumetric flow ratio of 1:9, 1:4, 1:1, 4:1, and 9:1. It was found that the methane conversion given by 5%Pr-Ni/MgO with the CO_2/CH_4 of 1:1 was the highest than the other flow ratio of 61.4%. The conversion reduces when the CO_2/CH_4 flow ration lower of higher than 1:1. %. It can be claimed that, there were no adequate amount of CO_2 to help resist the carbon deposition onto the catalyst when the CO_2/CH_4 volumetric flow ratio is less than 1:1. As the CO_2/CH_4 volumetric flow ratio is more than 1:1 also reduces the conversion due because the CH_4 in the inlet is low. The rate of formation of H_2 was decreasing when the CO_2/CH_4 volumetric flow ratio is increases. However, the CO formation shows quadratic trend where the peak CO rate of formation found when the CO_2/CH_4 flow ratio at 1:4. The rate law obtained respect to methane is given by

$$-r_{CH_4} = k\left[CH_{CH_4}\right]^{0.6111}\left[CO_2\right]^{0.42741}$$

Where k is $k = 0.372e^{-66.098/RT}$

The activation energy obtained on this reaction with 5% Pr-Ni/MgO was 66.098 kJ/mol.

The addition of Pr as increase the activation energy, E_a of the catalyst as the Pr is alkaline that induced the electron enrichment in Ni active site.

5.2 Recommendations

Several recommendation could be applied on further study on this methane dry reforming given by,

1. The catalyst should be reduced with N_2 and H_2 before the reaction activity conducted onto the particular catalyst to avoid the catalyst to consume product of the reaction.

2. Stainless steel of mesh type tray that has small mesh size than catalyst could be used instead of quartz wool that hold the catalyst and allows it well spread on the tray which will let the inlet gas to completely get access to the surface of the catalyst.
3. Gas mixer should be installed before the inlet reactant gas enter to the reactor to allow the gas homogenously mixed.
4. Preheating the inlet gas could be useful before let the inlet gas entering the reactor to allow the reactant to reach the desired reaction temperature as it could reduce the error.

5.3 Future studies recommendation

1. Different type of reactor on methane dry reforming over the same promoted alkaline earth metal catalyst like multi-phase reactor, fluidized bed reactor or membrane reactor can be studied to investigate the reactor type toward the activity of the catalyst.

2. Calcination temperature on the catalyst effect onto the reaction activity should be also studied to investigate the morphology of the catalyst toward the calcination temperature.

3. Double promoter onto the catalyst instead of bimetallic actives metal should be studied over the same catalyst for methane dry reforming.

4. Carbon deposition onto the double promoted alkaline earth metal on Ni catalyst study could be useful information as a backbone on selecting the catalyst for further research.

5. Study on methane reforming in liquid phase under high pressure and the heat transfer studies could be benefit to reduce the energy consumption to conduct the reaction.

References

Aasberg-Petersen, K., Dybkjær, I., Ovesen, C. V., Schjødt, N. C., Sehested, J., & Thomsen, S. G. (2011). Natural gas to synthesis gas – Catalysts and catalytic processes. *Journal of Natural Gas Science and Engineering*, *3*(2), 423–459. doi:10.1016/j.jngse.2011.03.004

Albarazi, A., Beaunier, P., & Da Costa, P. (2013). Hydrogen and syngas production by methane dry reforming on SBA-15 supported nickel catalysts: On the effect of promotion by Ce0.75Zr0.25O2 mixed oxide. *International Journal of Hydrogen Energy*, *38*(1), 127–139. doi:10.1016/j.ijhydene.2012.10.063

Azzam, K. G., Babich, I. V., Seshan, K., & Lefferts, L. (2008). Role of Re in Pt–Re/TiO2 catalyst for water gas shift reaction: A mechanistic and kinetic study. *Applied Catalysis B: Environmental*, *80*(1-2), 129–140. doi:10.1016/j.apcatb.2007.11.015

Bradford, M. C. J., & Albert, M. V. (1996). A : Catalytic reforming of methane with carbon dioxide over nickel catalysts II . Reaction kinetics, *142*, 97–122.

Chin, M. J., Poh, P. E., Tey, B. T., Chan, E. S., & Chin, K. L. (2013). Biogas from palm oil mill effluent (POME): Opportunities and challenges from Malaysia's perspective. *Renewable and Sustainable Energy Reviews*, *26*, 717–726. doi:10.1016/j.rser.2013.06.008

Damyanova, S., Pawelec, B., Arishtirova, K., & Fierro, J. L. G. (2012). Ni-based catalysts for reforming of methane with CO2. *International Journal of Hydrogen Energy*, *37*(21), 15966–15975. doi:10.1016/j.ijhydene.2012.08.056

Darujati, A. R. S., & Thomson, W. J. (2006). Kinetic study of a ceria-promoted catalyst in dry-methane reforming. *Chemical Engineering Science*, *61*(13), 4309–4315. doi:10.1016/j.ces.2006.02.007

Deutschmann. (2011). Catalytic dry reforming of methane, *54*, 327856.

Djaidja, a., Libs, S., Kiennemann, a., & Barama, a. (2006). Characterization and activity in dry reforming of methane on NiMg/Al and Ni/MgO catalysts. *Catalysis Today*, *113*(3-4), 194–200. doi:10.1016/j.cattod.2005.11.066

Feng, J., Ding, Y., Guo, Y., Li, X., & Li, W. (2013). Calcination temperature effect on the adsorption and hydrogenated dissociation of CO2 over the NiO/MgO catalyst. *Fuel*, *109*, 110–115. doi:10.1016/j.fuel.2012.08.028

Frusteri, F., Arena, F., Calogero, G., Torre, T., & Parmaliana, a. (2001). Potassium-enhanced stability of Ni/MgO catalysts in the dry-reforming of methane. *Catalysis Communications*, *2*(2), 49–56. doi:10.1016/S1566-7367(01)00008-5

García, V., Fernández, J. J., Ruíz, W., Mondragón, F., & Moreno, A. (2009). Effect of MgO addition on the basicity of Ni/ZrO2 and on its catalytic activity in carbon dioxide reforming of methane. *Catalysis Communications*, *11*(4), 240–246. doi:10.1016/j.catcom.2009.10.003

Juan-Juan, J., Román-Martínez, M. C., & Illán-Gómez, M. J. (2006). Effect of potassium content in the activity of K-promoted Ni/Al2O3 catalysts for the dry reforming of methane. *Applied Catalysis A: General*, *301*(1), 9–15. doi:10.1016/j.apcata.2005.11.006

Kaewmai, R., H-Kittikun, A., & Musikavong, C. (2012). Greenhouse gas emissions of palm oil mills in Thailand. *International Journal of Greenhouse Gas Control*, *11*, 141–151. doi:10.1016/j.ijggc.2012.08.006

Khajenoori, M., Rezaei, M., & Meshkani, F. (2014). Dry reforming over CeO2-promoted Ni/MgO nano-catalyst: Effect of Ni loading and CH4/CO2 molar ratio. *Journal of Industrial and Engineering Chemistry*, 6–11. doi:10.1016/j.jiec.2014.03.043

Meshkani, F., & Rezaei, M. (2010). Nanocrystalline MgO supported nickel-based bimetallic catalysts for carbon dioxide reforming of methane. *International Journal of Hydrogen Energy*, *35*(19), 10295–10301. doi:10.1016/j.ijhydene.2010.07.138

Meshkani, F., & Rezaei, M. (2011). Ni catalysts supported on nanocrystalline magnesium oxide for syngas production by CO2 reforming of CH4. *Journal of Natural Gas Chemistry*, *20*(2), 198–203. doi:10.1016/S1003-9953(10)60169-7

Meshkani, F., Rezaei, M., & Andache, M. (2013). Investigation of the catalytic performance of Ni/MgO catalysts in partial oxidation, dry reforming and combined reforming of methane. *Journal of Industrial and Engineering Chemistry*. doi:10.1016/j.jiec.2013.06.052

Ni, J., Chen, L., Lin, J., Schreyer, M. K., Wang, Z., & Kawi, S. (2013). High performance of Mg–La mixed oxides supported Ni catalysts for dry reforming of methane: The effect of crystal structure. *International Journal of Hydrogen Energy*, *38*(31), 13631–13642. doi:10.1016/j.ijhydene.2013.08.041

Norton, C. suryanarayan. and M. G. (1998). *X-ray Diffraction A practical Approach* (1st Editio.). Plenum Publishing Corporation.

Özdemir, H., Öksüzömer, M. a. F., & Gürkaynak, M. A. (2014). Effect of the calcination temperature on Ni/MgAl2O4 catalyst structure and catalytic properties for partial oxidation of methane. *Fuel*, *116*, 63–70. doi:10.1016/j.fuel.2013.07.095

Özkara-Aydınoğlu, Ş., & Erhan Aksoylu, a. (2013). A comparative study on the kinetics of carbon dioxide reforming of methane over Pt–Ni/Al2O3 catalyst: Effect of Pt/Ni Ratio. *Chemical Engineering Journal*, *215-216*, 542–549. doi:10.1016/j.cej.2012.11.034

Pichas, C., Pomonis, P., Petrakis, D., & Ladavos, A. (2010). Applied Catalysis A : General Kinetic study of the catalytic dry reforming of CH 4 with CO 2 over La 2 − x Sr x NiO 4 perovskite-type oxides. *"Applied Catalysis A, General"*, *386*(1-2), 116–123. doi:10.1016/j.apcata.2010.07.043

Ruckenstein, E., & Hu, Y. H. (1996). Role of Support in CO 2 Reforming of CH 4 to Syngas over Ni Catalysts, *238*(0280), 230–238.

Rupani, P. F., Singh, R. P., Ibrahim, M. H., & Esa, N. (2010). Review of Current Palm Oil Mill Effluent (POME) Treatment Methods : Vermicomposting as a Sustainable Practice, *11*(1), 70–81.

Tottrup. (1976). Kinetics of Decomposition of Carbon Monoxide on a Supported Nickel Catalyst. *Journal of Catalysis*, *36*, 29–36.

Xu, L., Miao, Z., Song, H., & Chou, L. (2013). ScienceDirect CO 2 reforming of CH 4 over rare earth elements functionalized mesoporous Ni e Ln (Ln [Ce , La , Sm , Pr) e Al e O composite oxides. *International Journal of Hydrogen Energy*, *39*(7), 3253–3268. doi:10.1016/j.ijhydene.2013.12.077

Yacob, S., Ali, M., Shirai, Y., Wakisaka, M., & Subash, S. (2005). Baseline study of methane emission from open digesting tanks of palm oil mill effluent treatment, *59*, 1575–1581. doi:10.1016/j.chemosphere.2004.11.040

Yao, L., Zhu, J., Peng, X., Tong, D., & Hu, C. (2013). Comparative study on the promotion effect of Mn and Zr on the stability of Ni/SiO2 catalyst for CO2 reforming of methane. *International Journal of Hydrogen Energy*, *38*(18), 7268–7279. doi:10.1016/j.ijhydene.2013.02.126

Zanganeh, R., Rezaei, M., & Zamaniyan, A. (2013). Dry reforming of methane to synthesis gas on NiO–MgO nanocrystalline solid solution catalysts. *International Journal of Hydrogen Energy*, *38*(7), 3012–3018. doi:10.1016/j.ijhydene.2012.12.089

Zanganeh, R., Rezaei, M., & Zamaniyan, A. (2014). Preparation of nanocrystalline NiO–MgO solid solution powders as catalyst for methane reforming with carbon dioxide: Effect of preparation conditions. *Advanced Powder Technology*. doi:10.1016/j.apt.2014.02.015

Zhang, J., Xin, Z., Meng, X., & Tao, M. (2013). Synthesis, characterization and properties of anti-sintering nickel incorporated MCM-41 methanation catalysts. *Fuel*, *109*, 693–701. doi:10.1016/j.fuel.2013.03.037

Appendix A

EDX detailed result

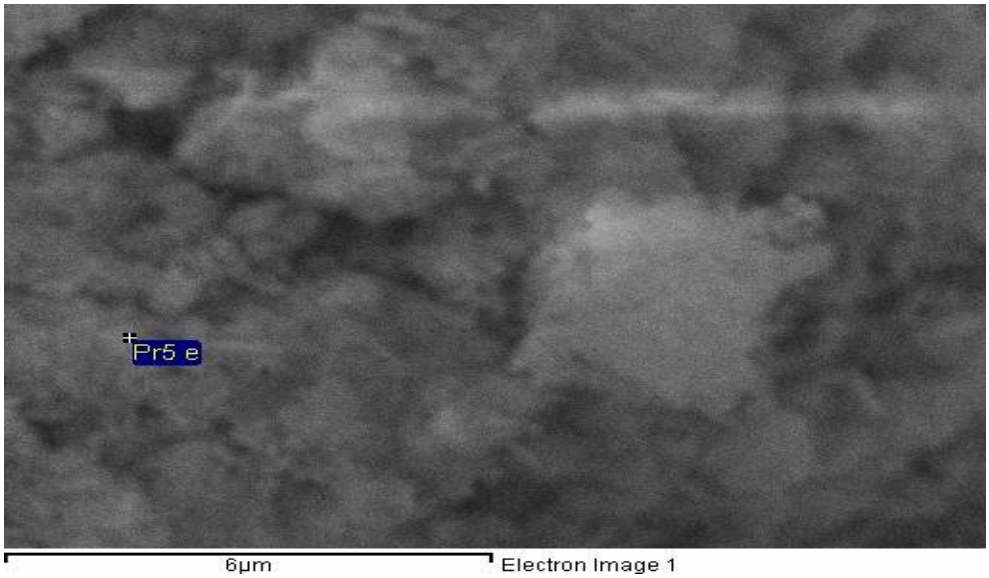

Spectrum processing:
Peaks possibly omitted: 2.069, 3.690, 9.440 keV

Processing option: Oxygen by stoichiometry (Normalised)
Number of iterations = 3

Standard :
C CaCO3 1-Jun-1999 12:00 AM
Mg MgO 1-Jun-1999 12:00 AM
Ni Ni 1-Jun-1999 12:00 AM
Cu Cu 1-Jun-1999 12:00 AM
Pr PrF3 1-Jun-1999 12:00 AM

Element	Weight%	Atomic%	Compd%	Formula
C K	8.41	14.61	30.82	CO2
Mg K	24.04	20.63	39.87	MgO
Ni K	18.37	6.53	23.38	NiO
Cu L	0.00	0.00	0.00	CuO
Pr L	5.07	0.75	5.94	Pr2O3
O	44.10	57.49		
Totals	100.00			

Appendix B

Finding the reactant concentration reaction order:

Initial Reactant CO_2 and CH_4 concentration of 5% Pr-Ni/MgO at different temperature with same inlet CH_4 and CO_2 concentration

Temperature,	CH_4 (Inlet) mol/l	$CO_{2(inlet)}$ mol/l
1073	0.002045	0.040897
1123	0.002045	0.040897
1173	0.002045	0.040897

Initial Reactant CO_2 and CH_4 concentration of 5% Pr-Ni/MgO at same temperature withvaries inlet CH_4 and CO_2 concentration

Temperature	$CH_{4(inlet)}$ mol/l	$CO_{2(inlet)}$ mol/l
1173	0.073614	0.008179
1173	0.065435	0.016359
1173	0.040897	0.040897
1173	0.016359	0.065435
1173	0.008179	0.073614

General rate law for this reaction is given by,

$$-r_{CH_4} = k[CH_4]^a[CO_2]^b$$

The k value must be same at constant temperature, initial rate of formation is used to calculate power order.

$$12.1042\times10^{-5} = k\left[0.073614\right]^a\left[0.008179\right]^b \qquad \text{Equation 1}$$

$$8.08757\times10^{-5} = k\left[0.008179\right]^a\left[0.073614\right]^b \qquad \text{Equation 2}$$

Dividing both equation:

$$1.4966 = \left[9.0\right]^a\left[0.111\right]^b \qquad \text{Equation 3}$$

By trial and error in excel,

a	b	$(9.0)^a$	$(0.111)^b$	$(9.0)^a(0.111)^b$
0.611	0.4274	3.828619	0.390815	1.4963

0.6111	0.42741	3.829461	0.390806	1.4966
0.6112	0.42742	3.830302	0.390798	1.4969
0.6113	0.42743	3.831144	0.390789	1.4972
0.6114	0.42744	3.831986	0.39078	1.4975
0.6115	0.42745	3.832828	0.390772	1.4978
0.6116	0.42746	3.83367	0.390763	1.4981
0.6117	0.42747	3.834512	0.390755	1.4984
0.6118	0.42748	3.835355	0.390746	1.4987
0.6119	0.42749	3.836198	0.390738	1.4989
0.612	0.4275	3.837041	0.390729	1.4992

Therefore, the obtained power order is 0.6111 for CH_4 and 0.42741 for CO_2

Appendix C

Data of the previous literature used to plot figure 2.3, figure 2.4 and figure 2.5

Figure 2.3

Catalyst	Carbon deposition ($mol/CH_{4\ converted}$)
5%Ni/10MgO-La_2O_3	0.031
5%Ni/5MgO-La_2O_3	0.035
5%Ni/3MgO-La_2O_3	0.035
5%Ni/MgO-La_2O_3	0.036
5%Ni/La_2O_3	0.048
5%Ni/20MgO-La_2O_3	0.550
5% Ni/MgO	1.400

Reference from:

Ni, Jun et al. 2013. "High Performance of Mg–La Mixed Oxides Supported Ni Catalysts for Dry Reforming of Methane: The Effect of Crystal Structure." *International Journal of Hydrogen Energy* 38(31):13631–42. Retrieved October 7, 2013 (http://linkinghub.elsevier.com/retrieve/pii/S0360319913019812).

Figure 2.4

Catalyst	Carbon formation ,$mol/(CO2 +CH4)_{(converted)}$
$Ni_{0.05}Al_{0.95}$	0.000013
$Ni_{0.05}Mg_{0.95}$	0.000033
2Mg/Al	0.000042
5% Ni/MgO	0.000064
2($Ni_{0.05}Mg_{0.95}$)/Al	0.00011
2($Ni_{0.1}Mg_{0.9}$)/Al	0.00011

Reference from:

Djaidja, a., S. Libs, a. Kiennemann, and a. Barama. 2006. "Characterization and Activity in Dry Reforming of Methane on NiMg/Al and Ni/MgO Catalysts."

Catalysis Today 113(3-4):194–200. Retrieved May 16, 2014 (http://linkinghub.elsevier.com/retrieve/pii/S0920586105008874).

Figure 2.5

Catalyst	carbon deposition mg C/mg(cat)
Ni/ZrO_2–0.4% MgO	0.26
Ni/ZrO_2–2.3% MgO	0.26
Ni/ZrO_2–1.2% MgO	0.31
Ni/ZrO_2	0.8

Reference From:

García, Verónica, Jhon J. Fernández, Wilson Ruíz, Fanor Mondragón, and Andrés Moreno. 2009. "Effect of MgO Addition on the Basicity of Ni/ZrO2 and on Its Catalytic Activity in Carbon Dioxide Reforming of Methane." *Catalysis Communications* 11(4):240–46. Retrieved May 16, 2014 (http://linkinghub.elsevier.com/retrieve/pii/S1566736709003707).

Appendix D

Catalyst Preparation:

1. **50 g of 20% Ni/MgO**

20% Ni : 80% MgO

Amount of Ni : $\frac{20}{100} \times 50g = 10g$

Amount of MgO: $\frac{80}{100} \times 50 = 40g$

Molar mass of $Ni(NO_3)_2.6H_2O$ = 290.8 g/mol

Molar mass of Ni = 58.6 g/mol

$\frac{290.8g/mol}{58.6g/mol} \times 10g = 4.9624g$

Therefore, 4.9624g of $Ni(NO_3)_2.6H_2O$ required to be mixed with 40g of MgO.

2. **50 g of 1% Pr- 20%Ni/79%MgO**

Amount of Praseodymium: $0.01 \times 50g = 0.5g$

Amount of Ni : $\frac{20}{100} \times 50g = 10g$

Amount of MgO: $\frac{79}{100} \times 50 = 39.5g$

Molar mass of $Pr(NO_3)_3.6H_2O$ = 435.01 g/mol

Molar mass of Pr = 140.9 g/mol

$\frac{435.01g/mol}{140.9g/mol} \times 0.5g = 1.5437g$ of $Pr(NO_3)_3.6H_2O$ required.

Molar mass of $Ni(NO_3)_2.6H_2O$ = 290.8 g/mol

Molar mass of Ni = 58.6 g/mol

$$\frac{290.8g/mol}{58.6g/mol} \times 10g = 4.9624g$$

Therefore, to prepare 1% Pr-20% Ni/ 79% MgO 1.5437g of $Pr(NO_3)_3.6H_2O$, 4.9624g of $Ni(NO_3)_2.6H_2O$ and 39.5g of MgO required.

3. 50 g of 3% Pr- 20%Ni/77%MgO

Amount of Praseodymium: $0.03 \times 50g = 1.5g$

Amount of Ni : $\frac{20}{100} \times 50g = 10g$

Amount of MgO: $\frac{77}{100} \times 50 = 38.5g$

Molar mass of $Pr(NO_3)_3.6H_2O$ = 435.01 g/mol

Molar mass of Pr = 140.9 g/mol

$\frac{435.01g/mol}{140.9g/mol} \times 1.5g = 4.6311g$ of $Pr(NO_3)_3.6H_2O$ required.

Molar mass of $Ni(NO_3)_2.6H_2O$ = 290.8 g/mol

Molar mass of Ni = 58.6 g/mol

$$\frac{290.8g/mol}{58.6g/mol} \times 10g = 4.9624g$$

Therefore, to prepare 3% Pr-20% Ni/ 79% MgO 4.6311g of $Pr(NO_3)_3.6H_2O$, 4.9624g of $Ni(NO_3)_2.6H_2O$ and 38.5g of MgO required.

4. 50 g of 5% Pr- 20%Ni/77%MgO

Amount of Praseodymium: $0.05 \times 50g = 2.5g$

Amount of Ni : $\frac{20}{100} \times 50g = 10g$

Amount of MgO: $\frac{75}{100} \times 50 = 37.5g$

Molar mass of $Pr(NO_3)_3.6H_2O$ = 435.01 g/mol

Molar mass of Pr = 140.9 g/mol

$\frac{435.01 g/mol}{140.9 g/mol} \times 2.5 g = 7.7184 g$ of $Pr(NO_3)_3.6H_2O$ required.

Molar mass of $Ni(NO_3)_2.6H_2O$ = 290.8 g/mol

Molar mass of Ni = 58.6 g/mol

$\frac{290.8 g/mol}{58.6 g/mol} \times 10 g = 4.9624 g$

Therefore, to prepare 3% Pr-20% Ni/ 79% MgO 7.7184g of $Pr(NO_3)_3.6H_2O$, 4.9624g of $Ni(NO_3)_2.6H_2O$ and 37.5g of MgO required.

Appendix E

Catalyst screening data via methane conversion at CO_2/CH_4 volumetric flow ratio of 1:1.

Catalyst	20% Ni/MgO
Reactant Flow rate ratio	1:1
Temperature, °C	Conversion, X
1073.00	12.5592
1123.00	15.8724
1173.00	23.6378

Catalyst	1 % Pr
Flow rate ratio	1:1
Temperature, °C	Conversion, X
1073.00	12.1199
1123.00	15.6925
1173.00	23.3184

Catalyst	3 % Pr
Flow rate ratio	1:1
Temperature, °C	Conversion, X
1073.00	16.0280
1123.00	17.8782
1173.00	40.3449

Catalyst	5 % Pr
Flow rate ratio	1:1
Temperature, °C	Conversion, X
1073.00	16.7235
1123.00	19.5335
1173.00	61.4351

Methane conversion data of 5% Pr-Ni/MgO at 900°C with CO_2/CH_4 varies volumetric flow ratio parameter.

Catalyst	5 % Pr
Temperature, °C	900
Reactant flow ratio, CO_2/CH_4	Conversion, X
0.11	40.8060
0.25	55.5051
1.00	61.4351
4.00	22.5646
9.00	17.6673